EXTENDED EXPERIMENTAL PROCEDURES

See Table S3 for a list of all DNA constructs and peptides used in this study.

Protein Purification:

Different forms of human or drosophila WRC were purified essentially as previously described for the mini-WRC (Chen et al., 2010; Ismail et al., 2009). Briefly, MBP tagged WAVE1, Abi2 and HSPC300 were separately expressed in BL21 (DE3) T1^{R} and purified using amylose affinity beads (New England Biolabs) in the lysis buffer (20 mM Tris-HCl, 200 mM NaCl, 1 mM EDTA and 5mM beta-mercaptoethanol, pH8.5). The MBP-tagged WAVE1-H6-FL was expressed in ArcticExpress^{TM} (DE3)RIL cells (Stratagene) at 10 °C and purified by amylose affinity beads followed by Ni-NTA affinity beads to remove truncated proteins. Purified WAVE1, Abi2 and HSPC300 were then mixed in the presence of 1% (w/v) NP40 (plus 2 M urea for drosophila proteins), and protease inhibitors overnight at 4 °C to form a WAVE1/Abi2/HSPC300 trimeric subcomplex, which was further purified by a Source Q15 column (GE Healthcare). His_6 tagged Sra1 and Nap1 were expressed in SF9 and Hi5 cells, respectively. The cells were co-lysed in WRC buffer (20 mM Tris-HCl, 200 mM NaCl, 20% (w/v) glycerol, and 5 mM beta-mercaptoethanol, pH 8.5) by one cycle of slow freezing/thawing in ice water to produce the Sra1/Nap1 dimeric subcomplex, which was purified using Ni-NTA agarose beads (Qiagen) and a Source Q15 column. The WAVE1/Abi2/HSPC300 trimer was then mixed with the Sra1/Nap1 dimer and further purified by amylose affinity beads to remove excess dimer. For drosophila WRC, an additional Ni NTA affinity purification was used to remove unincorporated trimer. The resulting WRC pentamer was treated with Tev

protease to remove the MBP and His_6 tags and finally purified by Source Q15 column and Superdex200 columns. For the di-MBP (2MBP) tagged WRC, the 2MBP tag was not removed as 2MBP-HSPC300 lacks a Tev cleavage site.

GST tagged cytoplasmic tails of different transmembrane proteins were expressed in BL21 (DE3) $T1^R$ or ArcticExpress^{TM} (DE3)RIL cells and purified using glutathione sepharose beads. The proteins were either directly used for pull down assays or further purified using Source Q15 and/or Source SP15 columns and finally a superdex200 gel filtration column. Proteins used in pyrene-actin polymerization assays were treated with Tev protease to remove the GST tag and further purified by Source Q15 and/or Source SP15 columns and finally a superdex75 gel filtration column.

Other proteins, including Arp2/3 complex, actin, VCA, Rac1 and Tev protease, were purified as previously described (Ismail et al., 2009).

Pull-down Assays:

MBP pull down was performed by mixing 60 pmol of 2MBP tagged WRC and 5- to 10-fold excess prey proteins with 15 μL of amylose beads in 1 mL of binding buffer (20 mM HEPES, 120 mM NaCl, 5% (w/v) glycerol, 1 mM EDTA and 5 mM beta-mercaptoethanol, pH 7) at 4 °C for 30 min. The beads were centrifuged and washed three times. Bound proteins were eluted with 0.5% (w/v) maltose added in binding buffer, and examined by SDS-PAGE.

GST pull down was performed similarly, using 60 pmol of GST-tagged bait and 2-5 fold excess prey proteins with 20 μL of glutathione sepharose beads in 1 mL of binding buffer at 4 °C for 30 min, followed by three washes. Bound proteins were eluted with GST elution buffer (100 mM Tris-HCl, 120 mM NaCl, 5% (w/v) glycerol, 1 mM EDTA, 5 mM beta-mercaptoethanol and 30 mM reduced glutathione, pH 8.5) and examined by SDS-PAGE.

Mouse Brain Lysate Pull-down and Co-immunoprecipitation Assay:

Frozen whole brain (unstripped) from adult mouse (Pel-Freez Biologicals) was lysed on ice using a dounce homogenizer in 10 fold (v/w) of co-IP buffer (50 mM Tris-HCl, 150 mM NaCl, 5% (w/v) glycerol, 1% (w/v) NP40, 1 mM EDTA, 1 mM PMSF, 5 μg/mL Leupeptin, 5 μg/mL Antipain and 5 mM Benzamidine, pH 7.6), followed by rotary mixing at 4 °C for 1 hr. The brain lysate was clarified by centrifugation at 50 krpm (180 kg) in a Ti70 rotor at 4 °C for 1 hr. The clarified lysate was aliquoted and flash frozen. Before each experiment, an aliquot of lysate was thawed and clarified again by centrifuging at 16 kg at 4 °C for 10 min.

GST pull down from the mouse brain lysate was performed by mixing clarified lysate (containing 1 mg total protein measured by the BCA method) with 60 pmol of purified GST-mPCDH10 CT_{short} (879-1040) and 20 μL of glutathione sepharose beads in 0.5 mL of co-IP buffer at 4 °C for 1 hr. The beads were washed 3 times in a spin column and boiled in 50 μL of 2X SDS-PAGE buffer.

For co-immunoprecipitation, the brain lysate was pre-treated with protein A/G PLUS beads (Santa Cruz Biotech) at 4 °C for 1 hr. The pre-treated lysate (containing 1 mg of total protein) was mixed with 8 μg of anti-WAVE1 rabbit polyclonal antibody (Sigma-Aldrich, W0392), 10 μL of protein A/G PLUS beads in 0.5 mL of co-IP buffer at 4 °C for 1-2 hr or overnight. After washing the beads three times in a spin column, the bound proteins were eluted by gentle vortexing in 50 μL of co-IP buffer supplemented with 4 mM peptide A at 4 °C overnight. The eluted proteins were resolved by SDS-PAGE, transferred to PVDF membrane, and blotted for WAVE1 (Neuromab, clone K91/36), Sra1 (Upstate, 07-531), PCDH10 (Sigma-aldrich, HPA011220), or ROBO1 (Sigma-aldrich, SAB2501464).

The WIRS peptides (WT and AA) used for competition co-IP were synthesized by Abgent or the UTSW Protein Chemistry Core, and dissolved in 200 mM Tris-HCl, pH 7.6, with the final pH adjusted to 7 using NaOH. Both peptides were heated at 70 °C for ~5 minutes to aid dissolution. The dissolved peptides (25 mM for the WT and 20 mM for the AA) were filtered through a 0.2 μm pore-size syringe filter, aliquoted and flash frozen. Before use, the peptides were thawed and heated at 70 °C briefly.

The GST-hPCDH10 CT_{short} (879-1040, WT and AA) used for competition co-IP were purified by glutathione sepharose beads, and dialyzed against 20 mM Tris-HCl, 150 mM NaCl, 1 mM EDTA, 5% (w/v) glycerol, 1 μg/mL Leupeptin, 1 μg/mL antipain and 1 mM Benzamidine, pH 7.6. After spin-concentration in a 10-kDa MWCO concentrator (Amicon Ultra) to achieve >1 mM final concentrations, the proteins were aliquoted for

single use and flash frozen.

Protein Crystallography and X-ray Diffraction Data Collection:

Crystals of the WRC/WIRS complex were grown at 4 □C by hanging-drop vapor diffusion methods under similar conditions to those used previously for apo-miniWRC (Chen et al., 2010). The seleno-WIRS peptide (WGAERSM*STFGKEKA, M* = selenomethionine, synthesized by Abgent) was dissolved in degassed buffer (100 mM Tris-HCl, 50 mM NaCl, and 20 mM TCEP) at a final concentration of 26.5 mM, aliquoted and flash frozen. MiniWRC (~10 mg/ml or 30 μM, with Sra1 and Nap1 selenomethionine labeled) was mixed ~1:100 molar ratio with the seleno-WIRS peptide, and then mixed 1:1.8 (v/v) with mother liquid containing 100 mM Tris-HCl, 10 % (w/v) glycerol, 4 % PEG 10,000, 12-20 % PEG 300, 2 mM TCEP and 2 mM EDTA, pH 8.5. Crystals grew in the $P2_12_12_1$ space group and diffracted to 2.43 Å at the ID19 beamline at the Advanced Photon Source, Chicago. Data were processed and scaled using the HKL3000 suite (Minor et al., 2006).

Phase Determination and Structure Refinement:

The initial phases of the WRC/WIRS complex were determined by molecular replacement from the structure of the apo miniWRC, using the program suite PHENIX (Adams et al., 2010). The structural model was manually corrected with Coot (Emsley et al., 2010) and refined to R_{work}/R_{free} = 0.184/0.209 with PHENIX. Data collection and refinement statistics are shown in Table S2. The electron density for the WIRS peptide was verified by omit maps generated by PHENIX.

Isothermal Titration Calorimetry:

Proteins used for ITC (PCDH10 CT_{short} (879-1040) and 2MBP-miniWRC) were supplemented with 300 mM NaCl and concentrated using Amicon Ultra centrifuge concentrators. The proteins were then dialyzed against ITC buffer (20 mM Tris-HCl, 120 mM NaCl, 10% (w/v) glycerol, 1 mM EDTA and 1 mM DTT, pH 8.0) for three days. The ITC experiment was performed using a VP-ITC microcalorimeter (Microcal) at 20 °C, with 39.4 μM mPCDH10 CT_{short} titrated into 4 μM 2MBP-miniWRC. Data were analyzed and fit to a single-site binding model using Origin 7 (Microcal).

Fluorescence Anisotropy Measurement:

Fluorescence anisotropy assays were conducted using a PTI Fluorimeter (Photon Technology International). A synthetic FITC-labeled WIRS peptide (FITC-GAERSFSTFGKEKA) was used as the fluorescence anisotropy probe (λ_{ex} = 495 nm, λ_{em} = 521 nm). I_{vh} and I_{vv} were averaged from > 20 readings over 2 minutes. G factor was calculated as $G = (I_{hv\ samaple} - I_{hv\ buffer})/(I_{hh\ sample} - I_{hh\ buffer})$, and anisotropy was calculated using $r = (I_{vv} - G * I_{vh})/(I_{vv} + 2G * I_{vh})$. All protein samples were dialyzed or desalted into KMEI20Gd buffer (10 mM Imidazole, 50 mM KCl, 1 mM $MgCl_2$, 1 mM EGTA, 20% (w/v) glycerol and 1mM DTT, pH 7.0) before use. In direct binding measurement, 2MBP-ΔWRC was titrated into 50 nM FITC-WIRS in 200 μL of reaction. The anisotropy data were fit using a single-site 1:1 binding model to obtain K_D. In competition measurements, purified cytoplasmic tails of different WIRS proteins were titrated into 120 μL of reactions containing 350 nM 2MBP-ΔWRC and 50 nM FITC-WIRS . The

binding curves were fit to obtain the dissociation constant K_D using a complete solution for competitive binding to a single site on a receptor (Wang, 1995).

Beads Clustering Experiment:

NIH 3T3 cells stably expressing Sra1-YPet (Nguyen and Daugherty, 2005) were generated using MML (Moloney Murine Leukemia) viruses by standard procedures. Due to low expression levels of Sra1-YPet, stable cells were sorted to enrich for higher fluorescence (top 20% of cell population) using FACS (UTSW Flow Cytometry Core). The sorted cells were maintained and transfected using Lipofectamine 2000 (Invitrogen) to express CD16-CD7-CT-mCherry chimeric receptors (Kolanus et al., 1993), composed of the extracellular domain of CD16, the transmembrane domain of CD7, the cytoplasmic tail (CT) of PCDH10, PCDH17, or neuroligin1, and mCherry at the C terminus. At 24 hr post transfection, 1 μg/ml anti-human-CD16 monoclonal mouse antibody (Invitrogen) was added to cells for 1 hr. Cells were washed 2 times with pre-warmed medium before addition of $4.5x10^5$ Dynal beads (coated with M-280 Sheep anti-Mouse IgG (Invitrogen) washed with serum-free medium before use) per 1 mL of medium for 1 hr. Cells were fixed using 4% paraformaldehyde in cytoskeletal buffer solution (10 mM MES, 138 mM KCl, 10 mM EGTA, and 3 mM $MgCl_2$, pH 6.1) for 15 min at room temperature. Fixed cells were washed 4 times with PBS before mounting in Prolong Gold Antifade.

Imaging and Analysis:

Beads clustering chimeric receptors were imaged using a Zeiss LSM 510 Meta microscope, with 488 nm and 563 nm lasers for YPet and mCherry, respectively. Images

were line-averaged 8 times and Z-stacks spanning 1.6 mm were taken with Z-spacing of 0.4 mm. Images showing beads that clustered receptor-tails (enriched mCherry signal) were cropped and the best focal plane was chosen for blind-scoring by a naïve individual for whether the WRC was correspondingly recruited at the same focal plane (enriched YPet signal). An average of 40 total beads was imaged for the wild type tails and 20 for the mutant tails. The percentage of beads that successfully recruited Sra1-YPet was calculated (scored positive/total) and reported as an average from multiple experiments. Four to six repeats (n) of each experiment were performed for each receptor-tail. P values from Student's t-test were calculated using the program, R.

***Drosophila* Genetics:**

All strains and crosses were grown on *Drosophila* standard medium. All crosses were performed at 25 °C. The following strains were used (Stephan et al., 2011): FRT82B *abi*Δ20^{68E}, FRT82B *abi*Δ20, UAS-dAbi^{68E}, *elav*^{C155}Gal4 and *da*Gal4 (Boomington Stock Center). UAS-dAbi^{68E} wild type (WT), UAS-dAbi^{68E}-AW (R118A/G122W), UASp-dAbi^{68E}-WT and UASp-dAbi^{68E}-AW transgenes were generated by ΦC31-integrase-mediated integration into the landing site M{3xP3-RFP.attP'}ZH-68E (Bischof et al., 2007). Mutant dAbi (R118A/G122W) was generated by *in vitro* mutagenesis (Stratagene) of the Gateway Entry vector (Invitrogen) pENTR D-TOPO-dAbi using the following primers: R118A/G122W sense: AAG GAG AAG GTG GCC GCG AGA GAG ATT TGG GTG CTT ACG GCT AAC, and antisense: GTT AGC CGT AAG CAC CCA AAT CTC TCT CGC GGC CAC CTT CTC CTT. The mutant *abi* insert was sequenced and cloned into the pUASTattB rfA and pUASPattB rfA (*Drosophila* Genomics Resource

Center, DGRC), respectively by LR *in vitro* recombination (Invitrogen). Western blot analysis was used to examine the expression of dAbi and dWAVE in corresponding brains as previously described (Stephan et al., 2011). Essentially, equal amounts of protein lysates (from four brains) were separated by SDS-PAGE (10%) and blotted using rabbit α-dAbi (1:100, affinity purified polyclonal antibody raised against the C-terminal peptide of dAbi: SHIGMHTLGRNINR (Davids Biotechnology), guinea pig α-dWAVE (1:1000; Bogdan et al., 2005) or mouse α-tubulin (1:400, E7, Developmental Studies Hybridoma Bank). To test fertility, two females of indicated genotypes were mated with three wild type males. The number of offspring was counted after 15 days.

Immunohistochemistry:

Brains of third instar wandering larvae were dissected and stained as previously described (Stephan et al., 2011). Primary antibodies were used at the following dilutions: mouse mAB24B10: 1:40 (α-Chaoptin, Developmental Studies Hybridoma Bank), rabbit α-β-Galactosidase: 1:1000 (Cappel); rabbit α-mouse/rabbit-Alexa488/647: 1:1000 (Molecular Probes). Wild type ovaries (w^{1118}) and ovaries from rescued abiΔ20 mutant females (*abi*Δ20, *da*-Gal4/*abi*Δ20, UASp-dAbi-WT; and *abi*Δ20, *da*-Gal4/*abi*Δ20, UASp-dAbi-AW) were dissected in cold PBS, fixed in 4% paraformaldehyde in PBS for 20 min, and stained as previously described (Bogdan et al., 2005). The following fluorescent markers were used: Alexa-Fluor-488 phalloidin 1:100 (Invitrogen) and DAPI 1:1000 (Invitrogen). Fluorescent images were collected on a Zeiss (Jena, Germany) LSM510 confocal system with Zen software (Zen 2008). SIM images were obtained using an ELYRA S.1 Microscope (CellObserver SD, 63×/1.4 oil-immersion objective; Zeiss, Germany) with

Zen 2010 D. Images were processed with Adobe Photoshop and ImageJ. Quantification was performed in a blind fashion after 3D reconstruction.

SUPPLEMENTAL REFERENCES

Adams, P.D., Afonine, P.V., Bunkoczi, G., Chen, V.B., Davis, I.W., Echols, N., Headd, J.J., Hung, L.W., Kapral, G.J., Grosse-Kunstleve, R.W., *et al.* (2010). PHENIX: a comprehensive Python-based system for macromolecular structure solution. Acta Crystallogr D Biol Crystallogr *66*, 213-221.

Adrain, C., Zettl, M., Christova, Y., Taylor, N., and Freeman, M. (2012). Tumor necrosis factor signaling requires iRhom2 to promote trafficking and activation of TACE. Science *335*, 225-228.

Al Tassan, N., Khalil, D., Shinwari, J., Al Sharif, L., Bavi, P., Abduljaleel, Z., Abu Dhaim, N., Magrashi, A., Bobis, S., Ahmed, H., *et al.* (2012). A missense mutation in PIK3R5 gene in a family with ataxia and oculomotor apraxia. Hum Mutat *33*, 351-354.

Anastasio, N., Ben-Omran, T., Teebi, A., Ha, K.C., Lalonde, E., Ali, R., Almureikhi, M., Der Kaloustian, V.M., Liu, J., Rosenblatt, D.S., *et al.* (2010). Mutations in SCARF2 are responsible for Van Den Ende-Gupta syndrome. Am J Hum Genet *87*, 553-559.

Anitha, A., Nakamura, K., Yamada, K., Suda, S., Thanseem, I., Tsujii, M., Iwayama, Y., Hattori, E., Toyota, T., Miyachi, T., *et al.* (2008). Genetic analyses of roundabout (ROBO) axon guidance receptors in autism. Am J Med Genet B Neuropsychiatr Genet *147B*, 1019-1027.

Aruga, J., Yokota, N., and Mikoshiba, K. (2003). Human SLITRK family genes: genomic organization and expression profiling in normal brain and brain tumor tissue. Gene *315*, 87-94.

Asao, H., Sasaki, Y., Arita, T., Tanaka, N., Endo, K., Kasai, H., Takeshita, T., Endo, Y., Fujita, T., and Sugamura, K. (1997). Hrs is associated with STAM, a signal-transducing adaptor molecule. Its suppressive effect on cytokine-induced cell growth. J Biol Chem *272*, 32785-32791.

Ashburner, M., Ball, C.A., Blake, J.A., Botstein, D., Butler, H., Cherry, J.M., Davis, A.P., Dolinski, K., Dwight, S.S., Eppig, J.T., *et al.* (2000). Gene ontology: tool for the unification of biology. The Gene Ontology Consortium. Nat Genet *25*, 25-29.

Backx, L., Ceulemans, B., Vermeesch, J.R., Devriendt, K., and Van Esch, H. (2009). Early myoclonic encephalopathy caused by a disruption of the neuregulin-1 receptor ErbB4. Eur J Hum Genet *17*, 378-382.

Bahou, W.F., Campbell, A.D., and Wicha, M.S. (1992). cDNA cloning and molecular characterization of MSE55, a novel human serum constituent protein that displays bone marrow stromal/endothelial cell-specific expression. J Biol Chem *267*, 13986-13992.

Baig, S.M., Koschak, A., Lieb, A., Gebhart, M., Dafinger, C., Nurnberg, G., Ali, A., Ahmad, I., Sinnegger-Brauns, M.J., Brandt, N., *et al.* (2011). Loss of Ca(v)1.3 (CACNA1D) function in a human channelopathy with bradycardia and congenital deafness. Nat Neurosci *14*, 77-84.

Begni, S., Popoli, M., Moraschi, S., Bignotti, S., Tura, G.B., and Gennarelli, M. (2002). Association between the ionotropic glutamate receptor kainate 3 (GRIK3) ser310ala polymorphism and schizophrenia. Mol Psychiatry *7*, 416-418.
Berkel, S., Marshall, C.R., Weiss, B., Howe, J., Roeth, R., Moog, U., Endris, V., Roberts, W., Szatmari, P., Pinto, D., *et al.* (2010). Mutations in the SHANK2 synaptic scaffolding gene in autism spectrum disorder and mental retardation. Nat Genet *42*, 489-491.
Bernadskaya, Y.Y., Wallace, A., Nguyen, J., Mohler, W.A., and Soto, M.C. (2012). UNC-40/DCC, SAX-3/Robo, and VAB-1/Eph Polarize F-Actin during Embryonic Morphogenesis by Regulating the WAVE/SCAR Actin Nucleation Complex. PLoS Genet *8*, e1002863.
Bettler, B., Egebjerg, J., Sharma, G., Pecht, G., Hermans-Borgmeyer, I., Moll, C., Stevens, C.F., and Heinemann, S. (1992). Cloning of a putative glutamate receptor: a low affinity kainate-binding subunit. Neuron *8*, 257-265.
Bischof, J., Maeda, R.K., Hediger, M., Karch, F., and Basler, K. (2007). An optimized transgenesis system for Drosophila using germ-line-specific phiC31 integrases. Proc Natl Acad Sci U S A *104*, 3312-3317.
Blasutig, I.M., New, L.A., Thanabalasuriar, A., Dayarathna, T.K., Goudreault, M., Quaggin, S.E., Li, S.S., Gruenheid, S., Jones, N., and Pawson, T. (2008). Phosphorylated YDXV motifs and Nck SH2/SH3 adaptors act cooperatively to induce actin reorganization. Mol Cell Biol *28*, 2035-2046.
Blaydon, D.C., Etheridge, S.L., Risk, J.M., Hennies, H.C., Gay, L.J., Carroll, R., Plagnol, V., McRonald, F.E., Stevens, H.P., Spurr, N.K., *et al.* (2012). RHBDF2 mutations are associated with tylosis, a familial esophageal cancer syndrome. Am J Hum Genet *90*, 340-346.
Bogdan, S., Stephan, R., Lobke, C., Mertens, A., and Klambt, C. (2005). Abi activates WASP to promote sensory organ development. Nat Cell Biol *7*, 977-984.
Bogerd, H.P., Fridell, R.A., Madore, S., and Cullen, B.R. (1995). Identification of a novel cellular cofactor for the Rev/Rex class of retroviral regulatory proteins. Cell *82*, 485-494.
Bolliger, M.F., Martinelli, D.C., and Sudhof, T.C. (2011). The cell-adhesion G protein-coupled receptor BAI3 is a high-affinity receptor for C1q-like proteins. Proc Natl Acad Sci U S A *108*, 2534-2539.
Bolliger, M.F., Pei, J., Maxeiner, S., Boucard, A.A., Grishin, N.V., and Sudhof, T.C. (2008). Unusually rapid evolution of Neuroligin-4 in mice. Proc Natl Acad Sci U S A *105*, 6421-6426.
Bonora, E., Lamb, J.A., Barnby, G., Sykes, N., Moberly, T., Beyer, K.S., Klauck, S.M., Poustka, F., Bacchelli, E., Blasi, F., *et al.* (2005). Mutation screening and association analysis of six candidate genes for autism on chromosome 7q. Eur J Hum Genet *13*, 198-207.
Brugada, R., Hong, K., Dumaine, R., Cordeiro, J., Gaita, F., Borggrefe, M., Menendez, T.M., Brugada, J., Pollevick, G.D., Wolpert, C., *et al.* (2004). Sudden death associated with short-QT syndrome linked to mutations in HERG. Circulation *109*, 30-35.
Burbelo, P.D., Snow, D.M., Bahou, W., and Spiegel, S. (1999). MSE55, a Cdc42 effector protein, induces long cellular extensions in fibroblasts. Proc Natl Acad Sci U S A *96*, 9083-9088.
Busst, C.J., Bloomer, L.D., Scurrah, K.J., Ellis, J.A., Barnes, T.A., Charchar, F.J., Braund, P., Hopkins, P.N., Samani, N.J., Hunt, S.C., *et al.* (2011). The epithelial sodium channel

gamma-subunit gene and blood pressure: family based association, renal gene expression, and physiological analyses. Hypertension *58*, 1073-1078.
Castermans, D., Wilquet, V., Parthoens, E., Huysmans, C., Steyaert, J., Swinnen, L., Fryns, J.P., Van de Ven, W., and Devriendt, K. (2003). The neurobeachin gene is disrupted by a translocation in a patient with idiopathic autism. J Med Genet *40*, 352-356.
Channavajhala, P.L., Wu, L., Cuozzo, J.W., Hall, J.P., Liu, W., Lin, L.L., and Zhang, Y. (2003). Identification of a novel human kinase supporter of Ras (hKSR-2) that functions as a negative regulator of Cot (Tpl2) signaling. J Biol Chem *278*, 47089-47097.
Chen, Z., Borek, D., Padrick, S.B., Gomez, T.S., Metlagel, Z., Ismail, A.M., Umetani, J., Billadeau, D.D., Otwinowski, Z., and Rosen, M.K. (2010). Structure and control of the actin regulatory WAVE complex. Nature *468*, 533-538.
Cid, L.P., Montrose-Rafizadeh, C., Smith, D.I., Guggino, W.B., and Cutting, G.R. (1995). Cloning of a putative human voltage-gated chloride channel (CIC-2) cDNA widely expressed in human tissues. Hum Mol Genet *4*, 407-413.
Consortium, T.U. (2012). Reorganizing the protein space at the Universal Protein Resource (UniProt). Nucleic Acids Res *40*, D71-75.
Costa, G.L., Benson, J.M., Seroogy, C.M., Achacoso, P., Fathman, C.G., and Nolan, G.P. (2000). Targeting rare populations of murine antigen-specific T lymphocytes by retroviral transduction for potential application in gene therapy for autoimmune disease. J Immunol *164*, 3581-3590.
Curran, M.E., Splawski, I., Timothy, K.W., Vincent, G.M., Green, E.D., and Keating, M.T. (1995). A molecular basis for cardiac arrhythmia: HERG mutations cause long QT syndrome. Cell *80*, 795-803.
Dallol, A., Forgacs, E., Martinez, A., Sekido, Y., Walker, R., Kishida, T., Rabbitts, P., Maher, E.R., Minna, J.D., and Latif, F. (2002). Tumour specific promoter region methylation of the human homologue of the Drosophila Roundabout gene DUTT1 (ROBO1) in human cancers. Oncogene *21*, 3020-3028.
Dallosso, A.R., Hancock, A.L., Szemes, M., Moorwood, K., Chilukamarri, L., Tsai, H.H., Sarkar, A., Barasch, J., Vuononvirta, R., Jones, C., *et al.* (2009). Frequent long-range epigenetic silencing of protocadherin gene clusters on chromosome 5q31 in Wilms' tumor. PLoS Genet *5*, e1000745.
De Souza, A.T., Hankins, G.R., Washington, M.K., Orton, T.C., and Jirtle, R.L. (1995). M6P/IGF2R gene is mutated in human hepatocellular carcinomas with loss of heterozygosity. Nat Genet *11*, 447-449.
Deguchi, M., Hata, Y., Takeuchi, M., Ide, N., Hirao, K., Yao, I., Irie, M., Toyoda, A., and Takai, Y. (1998). BEGAIN (brain-enriched guanylate kinase-associated protein), a novel neuronal PSD-95/SAP90-binding protein. J Biol Chem *273*, 26269-26272.
Depienne, C., Bouteiller, D., Keren, B., Cheuret, E., Poirier, K., Trouillard, O., Benyahia, B., Quelin, C., Carpentier, W., Julia, S., *et al.* (2009). Sporadic infantile epileptic encephalopathy caused by mutations in PCDH19 resembles Dravet syndrome but mainly affects females. PLoS Genet *5*, e1000381.
Depienne, C., Cincotta, M., Billot, S., Bouteiller, D., Groppa, S., Brochard, V., Flamand, C., Hubsch, C., Meunier, S., Giovannelli, F., *et al.* (2011a). A novel DCC mutation and genetic heterogeneity in congenital mirror movements. Neurology *76*, 260-264.
Depienne, C., Trouillard, O., Bouteiller, D., Gourfinkel-An, I., Poirier, K., Rivier, F., Berquin, P., Nabbout, R., Chaigne, D., Steschenko, D., *et al.* (2011b). Mutations and

deletions in PCDH19 account for various familial or isolated epilepsies in females. Hum Mutat *32*, E1959-1975.
Derivery, E., Sousa, C., Gautier, J.J., Lombard, B., Loew, D., and Gautreau, A. (2009). The Arp2/3 activator WASH controls the fission of endosomes through a large multiprotein complex. Dev Cell *17*, 712-723.
Devarajan, P., Scaramuzzino, D.A., and Morrow, J.S. (1994). Ankyrin binds to two distinct cytoplasmic domains of Na,K-ATPase alpha subunit. Proc Natl Acad Sci U S A *91*, 2965-2969.
Dibbens, L.M., Tarpey, P.S., Hynes, K., Bayly, M.A., Scheffer, I.E., Smith, R., Bomar, J., Sutton, E., Vandeleur, L., Shoubridge, C., *et al.* (2008). X-linked protocadherin 19 mutations cause female-limited epilepsy and cognitive impairment. Nat Genet *40*, 776-781.
Dietz, M.L., Bernaciak, T.M., Vendetti, F., Kielec, J.M., and Hildebrand, J.D. (2006). Differential actin-dependent localization modulates the evolutionarily conserved activity of Shroom family proteins. J Biol Chem *281*, 20542-20554.
Ding, L., Getz, G., Wheeler, D.A., Mardis, E.R., McLellan, M.D., Cibulskis, K., Sougnez, C., Greulich, H., Muzny, D.M., Morgan, M.B., *et al.* (2008). Somatic mutations affect key pathways in lung adenocarcinoma. Nature *455*, 1069-1075.
Doi, H., Yoshida, K., Yasuda, T., Fukuda, M., Fukuda, Y., Morita, H., Ikeda, S., Kato, R., Tsurusaki, Y., Miyake, N., *et al.* (2011). Exome sequencing reveals a homozygous SYT14 mutation in adult-onset, autosomal-recessive spinocerebellar ataxia with psychomotor retardation. Am J Hum Genet *89*, 320-327.
Donoviel, D.B., Freed, D.D., Vogel, H., Potter, D.G., Hawkins, E., Barrish, J.P., Mathur, B.N., Turner, C.A., Geske, R., Montgomery, C.A., *et al.* (2001). Proteinuria and perinatal lethality in mice lacking NEPH1, a novel protein with homology to NEPHRIN. Mol Cell Biol *21*, 4829-4836.
Du, Y., Weed, S.A., Xiong, W.C., Marshall, T.D., and Parsons, J.T. (1998). Identification of a novel cortactin SH3 domain-binding protein and its localization to growth cones of cultured neurons. Mol Cell Biol *18*, 5838-5851.
Dunlop, M.G., Dobbins, S.E., Farrington, S.M., Jones, A.M., Palles, C., Whiffin, N., Tenesa, A., Spain, S., Broderick, P., Ooi, L.Y., *et al.* (2012). Common variation near CDKN1A, POLD3 and SHROOM2 influences colorectal cancer risk. Nat Genet *44*, 770-776.
Dyomin, V.G., Chaganti, S.R., Dyomina, K., Palanisamy, N., Murty, V.V., Dalla-Favera, R., and Chaganti, R.S. (2002). BCL8 is a novel, evolutionarily conserved human gene family encoding proteins with presumptive protein kinase A anchoring function. Genomics *80*, 158-165.
Emsley, P., Lohkamp, B., Scott, W.G., and Cowtan, K. (2010). Features and development of Coot. Acta Crystallogr D Biol Crystallogr *66*, 486-501.
Endele, S., Rosenberger, G., Geider, K., Popp, B., Tamer, C., Stefanova, I., Milh, M., Kortum, F., Fritsch, A., Pientka, F.K., *et al.* (2010). Mutations in GRIN2A and GRIN2B encoding regulatory subunits of NMDA receptors cause variable neurodevelopmental phenotypes. Nat Genet *42*, 1021-1026.
Erhardt, A., Czibere, L., Roeske, D., Lucae, S., Unschuld, P.G., Ripke, S., Specht, M., Kohli, M.A., Kloiber, S., Ising, M., *et al.* (2011). TMEM132D, a new candidate for

anxiety phenotypes: evidence from human and mouse studies. Mol Psychiatry *16*, 647-663.
Etournay, R., Zwaenepoel, I., Perfettini, I., Legrain, P., Petit, C., and El-Amraoui, A. (2007). Shroom2, a myosin-VIIa- and actin-binding protein, directly interacts with ZO-1 at tight junctions. J Cell Sci *120*, 2838-2850.
Faivre-Sarrailh, C., Falk, J., Pollerberg, E., Schachner, M., and Rougon, G. (1999). NrCAM, cerebellar granule cell receptor for the neuronal adhesion molecule F3, displays an actin-dependent mobility in growth cones. J Cell Sci *112 Pt 18*, 3015-3027.
Fearon, E.R., Cho, K.R., Nigro, J.M., Kern, S.E., Simons, J.W., Ruppert, J.M., Hamilton, S.R., Preisinger, A.C., Thomas, G., Kinzler, K.W., *et al.* (1990). Identification of a chromosome 18q gene that is altered in colorectal cancers. Science *247*, 49-56.
Feldmann, K.A., Pittelkow, M.R., Roche, P.C., Kumar, R., and Grande, J.P. (2001). Expression of an immediate early gene, IEX-1, in human tissues. Histochem Cell Biol *115*, 489-497.
Ferrell, R.E., Levinson, K.L., Esman, J.H., Kimak, M.A., Lawrence, E.C., Barmada, M.M., and Finegold, D.N. (1998). Hereditary lymphedema: evidence for linkage and genetic heterogeneity. Hum Mol Genet *7*, 2073-2078.
Franco, M., Peters, P.J., Boretto, J., van Donselaar, E., Neri, A., D'Souza-Schorey, C., and Chavrier, P. (1999). EFA6, a sec7 domain-containing exchange factor for ARF6, coordinates membrane recycling and actin cytoskeleton organization. EMBO J *18*, 1480-1491.
Gamba, G., Miyanoshita, A., Lombardi, M., Lytton, J., Lee, W.S., Hediger, M.A., and Hebert, S.C. (1994). Molecular cloning, primary structure, and characterization of two members of the mammalian electroneutral sodium-(potassium)-chloride cotransporter family expressed in kidney. J Biol Chem *269*, 17713-17722.
Garg, P., Verma, R., Nihalani, D., Johnstone, D.B., and Holzman, L.B. (2007). Neph1 cooperates with nephrin to transduce a signal that induces actin polymerization. Mol Cell Biol *27*, 8698-8712.
Geller, D.S., Farhi, A., Pinkerton, N., Fradley, M., Moritz, M., Spitzer, A., Meinke, G., Tsai, F.T., Sigler, P.B., and Lifton, R.P. (2000). Activating mineralocorticoid receptor mutation in hypertension exacerbated by pregnancy. Science *289*, 119-123.
Geller, D.S., Rodriguez-Soriano, J., Vallo Boado, A., Schifter, S., Bayer, M., Chang, S.S., and Lifton, R.P. (1998). Mutations in the mineralocorticoid receptor gene cause autosomal dominant pseudohypoaldosteronism type I. Nat Genet *19*, 279-281.
Giza, J., Urbanski, M.J., Prestori, F., Bandyopadhyay, B., Yam, A., Friedrich, V., Kelley, K., D'Angelo, E., and Goldfarb, M. (2010). Behavioral and cerebellar transmission deficits in mice lacking the autism-linked gene islet brain-2. J Neurosci *30*, 14805-14816.
Glessner, J.T., Wang, K., Cai, G., Korvatska, O., Kim, C.E., Wood, S., Zhang, H., Estes, A., Brune, C.W., Bradfield, J.P., *et al.* (2009). Autism genome-wide copy number variation reveals ubiquitin and neuronal genes. Nature *459*, 569-573.
GrandPre, T., Nakamura, F., Vartanian, T., and Strittmatter, S.M. (2000). Identification of the Nogo inhibitor of axon regeneration as a Reticulon protein. Nature *403*, 439-444.
Gregorio, S.P., Sallet, P.C., Do, K.A., Lin, E., Gattaz, W.F., and Dias-Neto, E. (2009). Polymorphisms in genes involved in neurodevelopment may be associated with altered brain morphology in schizophrenia: preliminary evidence. Psychiatry Res *165*, 1-9.

Grimm, C., Kraft, R., Sauerbruch, S., Schultz, G., and Harteneck, C. (2003). Molecular and functional characterization of the melastatin-related cation channel TRPM3. J Biol Chem *278*, 21493-21501.
Grumet, M., Mauro, V., Burgoon, M.P., Edelman, G.M., and Cunningham, B.A. (1991). Structure of a new nervous system glycoprotein, Nr-CAM, and its relationship to subgroups of neural cell adhesion molecules. J Cell Biol *113*, 1399-1412.
Gudmundsson, J., Sulem, P., Gudbjartsson, D.F., Jonasson, J.G., Masson, G., He, H., Jonasdottir, A., Sigurdsson, A., Stacey, S.N., Johannsdottir, H., *et al.* (2012). Discovery of common variants associated with low TSH levels and thyroid cancer risk. Nat Genet *44*, 319-322.
Guo, D., Holmlund, C., Henriksson, R., and Hedman, H. (2004). The LRIG gene family has three vertebrate paralogs widely expressed in human and mouse tissues and a homolog in Ascidiacea. Genomics *84*, 157-165.
Haberg, K., Lundmark, R., and Carlsson, S.R. (2008). SNX18 is an SNX9 paralog that acts as a membrane tubulator in AP-1-positive endosomal trafficking. J Cell Sci *121*, 1495-1505.
Hagens, O., Dubos, A., Abidi, F., Barbi, G., Van Zutven, L., Hoeltzenbein, M., Tommerup, N., Moraine, C., Fryns, J.P., Chelly, J., *et al.* (2006). Disruptions of the novel KIAA1202 gene are associated with X-linked mental retardation. Hum Genet *118*, 578-590.
Hannula-Jouppi, K., Kaminen-Ahola, N., Taipale, M., Eklund, R., Nopola-Hemmi, J., Kaariainen, H., and Kere, J. (2005). The axon guidance receptor gene ROBO1 is a candidate gene for developmental dyslexia. PLoS Genet *1*, e50.
Hansson, J.H., Nelson-Williams, C., Suzuki, H., Schild, L., Shimkets, R., Lu, Y., Canessa, C., Iwasaki, T., Rossier, B., and Lifton, R.P. (1995). Hypertension caused by a truncated epithelial sodium channel gamma subunit: genetic heterogeneity of Liddle syndrome. Nat Genet *11*, 76-82.
Haruki, S., Imoto, I., Kozaki, K., Matsui, T., Kawachi, H., Komatsu, S., Muramatsu, T., Shimada, Y., Kawano, T., and Inazawa, J. (2010). Frequent silencing of protocadherin 17, a candidate tumour suppressor for esophageal squamous cell carcinoma. Carcinogenesis *31*, 1027-1036.
Hijazi, M.M., Thompson, E.W., Tang, C., Coopman, P., Torri, J.A., Yang, D., Mueller, S.C., and Lupu, R. (2000). Heregulin regulates the actin cytoskeleton and promotes invasive properties in breast cancer cell lines. Int J Oncol *17*, 629-641.
Hildebrand, J.D., and Soriano, P. (1999). Shroom, a PDZ domain-containing actin-binding protein, is required for neural tube morphogenesis in mice. Cell *99*, 485-497.
Hirano, S., Yan, Q., and Suzuki, S.T. (1999). Expression of a novel protocadherin, OL-protocadherin, in a subset of functional systems of the developing mouse brain. J Neurosci *19*, 995-1005.
Holmes, S.E., O'Hearn, E., Rosenblatt, A., Callahan, C., Hwang, H.S., Ingersoll-Ashworth, R.G., Fleisher, A., Stevanin, G., Brice, A., Potter, N.T., *et al.* (2001). A repeat expansion in the gene encoding junctophilin-3 is associated with Huntington disease-like 2. Nat Genet *29*, 377-378.
Hornbeck, P.V., Kornhauser, J.M., Tkachev, S., Zhang, B., Skrzypek, E., Murray, B., Latham, V., and Sullivan, M. (2012). PhosphoSitePlus: a comprehensive resource for

investigating the structure and function of experimentally determined post-translational modifications in man and mouse. Nucleic Acids Res *40*, D261-270.
Hummel, T., Leifker, K., and Klambt, C. (2000). The Drosophila HEM-2/NAP1 homolog KETTE controls axonal pathfinding and cytoskeletal organization. Genes Dev *14*, 863-873.
Hwang, P.M., Glatt, C.E., Bredt, D.S., Yellen, G., and Snyder, S.H. (1992). A novel K+ channel with unique localizations in mammalian brain: molecular cloning and characterization. Neuron *8*, 473-481.
Ichtchenko, K., Hata, Y., Nguyen, T., Ullrich, B., Missler, M., Moomaw, C., and Sudhof, T.C. (1995). Neuroligin 1: a splice site-specific ligand for beta-neurexins. Cell *81*, 435-443.
Imai, Y., Soda, M., Inoue, H., Hattori, N., Mizuno, Y., and Takahashi, R. (2001). An unfolded putative transmembrane polypeptide, which can lead to endoplasmic reticulum stress, is a substrate of Parkin. Cell *105*, 891-902.
Irrthum, A., Karkkainen, M.J., Devriendt, K., Alitalo, K., and Vikkula, M. (2000). Congenital hereditary lymphedema caused by a mutation that inactivates VEGFR3 tyrosine kinase. Am J Hum Genet *67*, 295-301.
Ishiguro, H., Liu, Q.R., Gong, J.P., Hall, F.S., Ujike, H., Morales, M., Sakurai, T., Grumet, M., and Uhl, G.R. (2006). NrCAM in addiction vulnerability: positional cloning, drug-regulation, haplotype-specific expression, and altered drug reward in knockout mice. Neuropsychopharmacology *31*, 572-584.
Ishii, J., Adachi, H., Aoki, J., Koizumi, H., Tomita, S., Suzuki, T., Tsujimoto, M., Inoue, K., and Arai, H. (2002). SREC-II, a new member of the scavenger receptor type F family, trans-interacts with SREC-I through its extracellular domain. J Biol Chem *277*, 39696-39702.
Isidor, B., Le Merrer, M., Exner, G.U., Pichon, O., Thierry, G., Guiochon-Mantel, A., David, A., Cormier-Daire, V., and Le Caignec, C. (2011a). Serpentine fibula-polycystic kidney syndrome caused by truncating mutations in NOTCH2. Hum Mutat *32*, 1239-1242.
Isidor, B., Lindenbaum, P., Pichon, O., Bezieau, S., Dina, C., Jacquemont, S., Martin-Coignard, D., Thauvin-Robinet, C., Le Merrer, M., Mandel, J.L., *et al.* (2011b). Truncating mutations in the last exon of NOTCH2 cause a rare skeletal disorder with osteoporosis. Nat Genet *43*, 306-308.
Ismail, A.M., Padrick, S.B., Chen, B., Umetani, J., and Rosen, M.K. (2009). The WAVE regulatory complex is inhibited. Nat Struct Mol Biol *16*, 561-563.
Jamain, S., Quach, H., Betancur, C., Rastam, M., Colineaux, C., Gillberg, I.C., Soderstrom, H., Giros, B., Leboyer, M., Gillberg, C., *et al.* (2003). Mutations of the X-linked genes encoding neuroligins NLGN3 and NLGN4 are associated with autism. Nat Genet *34*, 27-29.
Jamal, S.M., Basran, R.K., Newton, S., Wang, Z., and Milunsky, J.M. (2010). Novel de novo PCDH19 mutations in three unrelated females with epilepsy female restricted mental retardation syndrome. Am J Med Genet A *152A*, 2475-2481.
Jen, J.C., Chan, W.M., Bosley, T.M., Wan, J., Carr, J.R., Rub, U., Shattuck, D., Salamon, G., Kudo, L.C., Ou, J., *et al.* (2004). Mutations in a human ROBO gene disrupt hindbrain axon pathway crossing and morphogenesis. Science *304*, 1509-1513.

Jenkins, Z.A., van Kogelenberg, M., Morgan, T., Jeffs, A., Fukuzawa, R., Pearl, E., Thaller, C., Hing, A.V., Porteous, M.E., Garcia-Minaur, S., *et al.* (2009). Germline mutations in WTX cause a sclerosing skeletal dysplasia but do not predispose to tumorigenesis. Nat Genet *41*, 95-100.

Jun, G., Nicolaou, M., Morrison, M.A., Buros, J., Morgan, D.J., Radeke, M.J., Yonekawa, Y., Tsironi, E.E., Kotoula, M.G., Zacharaki, F., *et al.* (2011). Influence of ROBO1 and RORA on risk of age-related macular degeneration reveals genetically distinct phenotypes in disease pathophysiology. PLoS One *6*, e25775.

Kaiser, E., Forster, R., Wolf, I., Ebensperger, C., Kuehl, W.M., and Lipp, M. (1993). The G protein-coupled receptor BLR1 is involved in murine B cell differentiation and is also expressed in neuronal tissues. Eur J Immunol *23*, 2532-2539.

Kanetsky, P.A., Mitra, N., Vardhanabhuti, S., Li, M., Vaughn, D.J., Letrero, R., Ciosek, S.L., Doody, D.R., Smith, L.M., Weaver, J., *et al.* (2009). Common variation in KITLG and at 5q31.3 predisposes to testicular germ cell cancer. Nat Genet *41*, 811-815.

Kariyazono, H., Ohno, T., Khajoee, V., Ihara, K., Kusuhara, K., Kinukawa, N., Mizuno, Y., and Hara, T. (2004). Association of vascular endothelial growth factor (VEGF) and VEGF receptor gene polymorphisms with coronary artery lesions of Kawasaki disease. Pediatr Res *56*, 953-959.

Karkkainen, M.J., Ferrell, R.E., Lawrence, E.C., Kimak, M.A., Levinson, K.L., McTigue, M.A., Alitalo, K., and Finegold, D.N. (2000). Missense mutations interfere with VEGFR-3 signalling in primary lymphoedema. Nat Genet *25*, 153-159.

Kasnauskiene, J., Ciuladaite, Z., Preiksaitiene, E., Matuleviciene, A., Alexandrou, A., Koumbaris, G., Sismani, C., Pepalyte, I., Patsalis, P.C., and Kucinskas, V. (2012). A single gene deletion on 4q28.3: PCDH18--a new candidate gene for intellectual disability? Eur J Med Genet *55*, 274-277.

Kaufman, L., Hayashi, K., Ross, M.J., Ross, M.D., and Klotman, P.E. (2004). Sidekick-1 is upregulated in glomeruli in HIV-associated nephropathy. J Am Soc Nephrol *15*, 1721-1730.

Kaufman, L., Yang, G., Hayashi, K., Ashby, J.R., Huang, L., Ross, M.J., Klotman, M.E., and Klotman, P.E. (2007). The homophilic adhesion molecule sidekick-1 contributes to augmented podocyte aggregation in HIV-associated nephropathy. FASEB J *21*, 1367-1375.

Kim, J.H., Park, M., Yang, S.Y., Jeong, B.S., Yoo, H.J., Kim, J.W., Chung, J.H., and Kim, S.A. (2006). Association study of polymorphisms in N-methyl-D-aspartate receptor 2B subunits (GRIN2B) gene with Korean alcoholism. Neurosci Res *56*, 220-223.

Klingensmith, J., Yang, Y., Axelrod, J.D., Beier, D.R., Perrimon, N., and Sussman, D.J. (1996). Conservation of dishevelled structure and function between flies and mice: isolation and characterization of Dvl2. Mech Dev *58*, 15-26.

Kohmura, N., Senzaki, K., Hamada, S., Kai, N., Yasuda, R., Watanabe, M., Ishii, H., Yasuda, M., Mishina, M., and Yagi, T. (1998). Diversity revealed by a novel family of cadherins expressed in neurons at a synaptic complex. Neuron *20*, 1137-1151.

Kolanus, W., Romeo, C., and Seed, B. (1993). T cell activation by clustered tyrosine kinases. Cell *74*, 171-183.

Kottgen, A., Glazer, N.L., Dehghan, A., Hwang, S.J., Katz, R., Li, M., Yang, Q., Gudnason, V., Launer, L.J., Harris, T.B., *et al.* (2009). Multiple loci associated with indices of renal function and chronic kidney disease. Nat Genet *41*, 712-717.

Krugmann, S., Anderson, K.E., Ridley, S.H., Risso, N., McGregor, A., Coadwell, J., Davidson, K., Eguinoa, A., Ellson, C.D., Lipp, P., *et al.* (2002). Identification of ARAP3, a novel PI3K effector regulating both Arf and Rho GTPases, by selective capture on phosphoinositide affinity matrices. Mol Cell *9*, 95-108.
Kuniba, H., Yoshiura, K., Kondoh, T., Ohashi, H., Kurosawa, K., Tonoki, H., Nagai, T., Okamoto, N., Kato, M., Fukushima, Y., *et al.* (2009). Molecular karyotyping in 17 patients and mutation screening in 41 patients with Kabuki syndrome. J Hum Genet *54*, 304-309.
Kupershmidt, S., Yang, T., Chanthaphaychith, S., Wang, Z., Towbin, J.A., and Roden, D.M. (2002). Defective human Ether-a-go-go-related gene trafficking linked to an endoplasmic reticulum retention signal in the C terminus. J Biol Chem *277*, 27442-27448.
Lane, L., Argoud-Puy, G., Britan, A., Cusin, I., Duek, P.D., Evalet, O., Gateau, A., Gaudet, P., Gleizes, A., Masselot, A., *et al.* (2012). neXtProt: a knowledge platform for human proteins. Nucleic Acids Res *40*, D76-83.
Laumonnier, F., Bonnet-Brilhault, F., Gomot, M., Blanc, R., David, A., Moizard, M.P., Raynaud, M., Ronce, N., Lemonnier, E., Calvas, P., *et al.* (2004). X-linked mental retardation and autism are associated with a mutation in the NLGN4 gene, a member of the neuroligin family. Am J Hum Genet *74*, 552-557.
Law, A.J., Kleinman, J.E., Weinberger, D.R., and Weickert, C.S. (2007). Disease-associated intronic variants in the ErbB4 gene are related to altered ErbB4 splice-variant expression in the brain in schizophrenia. Hum Mol Genet *16*, 129-141.
Lawson-Yuen, A., Saldivar, J.S., Sommer, S., and Picker, J. (2008). Familial deletion within NLGN4 associated with autism and Tourette syndrome. Eur J Hum Genet *16*, 614-618.
Lee, N., Chen, J., Sun, L., Wu, S., Gray, K.R., Rich, A., Huang, M., Lin, J.H., Feder, J.N., Janovitz, E.B., *et al.* (2003). Expression and characterization of human transient receptor potential melastatin 3 (hTRPM3). J Biol Chem *278*, 20890-20897.
Li, M.Z., and Elledge, S.J. (2007). Harnessing homologous recombination in vitro to generate recombinant DNA via SLIC. Nat Methods *4*, 251-256.
Lim, S., Naisbitt, S., Yoon, J., Hwang, J.I., Suh, P.G., Sheng, M., and Kim, E. (1999). Characterization of the Shank family of synaptic proteins. Multiple genes, alternative splicing, and differential expression in brain and development. J Biol Chem *274*, 29510-29518.
Linardopoulou, E.V., Parghi, S.S., Friedman, C., Osborn, G.E., Parkhurst, S.M., and Trask, B.J. (2007). Human subtelomeric WASH genes encode a new subclass of the WASP family. PLoS Genet *3*, e237.
Ludwig, D., Lorenz, J., Dejana, E., Bohlen, P., Hicklin, D.J., Witte, L., and Pytowski, B. (2000). cDNA cloning, chromosomal mapping, and expression analysis of human VE-Cadherin-2. Mamm Genome *11*, 1030-1033.
Marazziti, D., Golini, E., Gallo, A., Lombardi, M.S., Matteoni, R., and Tocchini-Valentini, G.P. (1997). Cloning of GPR37, a gene located on chromosome 7 encoding a putative G-protein-coupled peptide receptor, from a human frontal brain EST library. Genomics *45*, 68-77.
Marini, C., Mei, D., Parmeggiani, L., Norci, V., Calado, E., Ferrari, A., Moreira, A., Pisano, T., Specchio, N., Vigevano, F., *et al.* (2010). Protocadherin 19 mutations in girls with infantile-onset epilepsy. Neurology *75*, 646-653.

Marshall, C.R., Noor, A., Vincent, J.B., Lionel, A.C., Feuk, L., Skaug, J., Shago, M., Moessner, R., Pinto, D., Ren, Y., *et al.* (2008). Structural variation of chromosomes in autism spectrum disorder. Am J Hum Genet *82*, 477-488.
Martens, N., Wery, M., Wang, P., Braet, F., Gertler, A., Hooghe, R., Vandenhaute, J., and Hooghe-Peters, E.L. (2004). The suppressor of cytokine signaling (SOCS)-7 interacts with the actin cytoskeleton through vinexin. Exp Cell Res *298*, 239-248.
Matuoka, K., Miki, H., Takahashi, K., and Takenawa, T. (1997). A novel ligand for an SH3 domain of the adaptor protein Nck bears an SH2 domain and nuclear signaling motifs. Biochem Biophys Res Commun *239*, 488-492.
McDaniell, R., Warthen, D.M., Sanchez-Lara, P.A., Pai, A., Krantz, I.D., Piccoli, D.A., and Spinner, N.B. (2006). NOTCH2 mutations cause Alagille syndrome, a heterogeneous disorder of the notch signaling pathway. Am J Hum Genet *79*, 169-173.
Meakin, S.O., MacDonald, J.I., Gryz, E.A., Kubu, C.J., and Verdi, J.M. (1999). The signaling adapter FRS-2 competes with Shc for binding to the nerve growth factor receptor TrkA. A model for discriminating proliferation and differentiation. J Biol Chem *274*, 9861-9870.
Meda, S.A., Narayanan, B., Liu, J., Perrone-Bizzozero, N.I., Stevens, M.C., Calhoun, V.D., Glahn, D.C., Shen, L., Risacher, S.L., Saykin, A.J., *et al.* (2012). A large scale multivariate parallel ICA method reveals novel imaging-genetic relationships for Alzheimer's disease in the ADNI cohort. Neuroimage *60*, 1608-1621.
Mells, G.F., Floyd, J.A., Morley, K.I., Cordell, H.J., Franklin, C.S., Shin, S.Y., Heneghan, M.A., Neuberger, J.M., Donaldson, P.T., Day, D.B., *et al.* (2011). Genome-wide association study identifies 12 new susceptibility loci for primary biliary cirrhosis. Nat Genet *43*, 329-332.
Meyerhardt, J.A., Look, A.T., Bigner, S.H., and Fearon, E.R. (1997). Identification and characterization of neogenin, a DCC-related gene. Oncogene *14*, 1129-1136.
Minor, W., Cymborowski, M., Otwinowski, Z., and Chruszcz, M. (2006). HKL-3000: the integration of data reduction and structure solution--from diffraction images to an initial model in minutes. Acta Crystallogr D Biol Crystallogr *62*, 859-866.
Miyake, A., Mochizuki, S., Yokoi, H., Kohda, M., and Furuichi, K. (1999). New ether-a-go-go K(+) channel family members localized in human telencephalon. J Biol Chem *274*, 25018-25025.
Mohler, P.J., Schott, J.J., Gramolini, A.O., Dilly, K.W., Guatimosim, S., duBell, W.H., Song, L.S., Haurogne, K., Kyndt, F., Ali, M.E., *et al.* (2003). Ankyrin-B mutation causes type 4 long-QT cardiac arrhythmia and sudden cardiac death. Nature *421*, 634-639.
Morrow, E.M., Yoo, S.Y., Flavell, S.W., Kim, T.K., Lin, Y., Hill, R.S., Mukaddes, N.M., Balkhy, S., Gascon, G., Hashmi, A., *et al.* (2008). Identifying autism loci and genes by tracing recent shared ancestry. Science *321*, 218-223.
Mutesa, L., Azad, A.K., Verhaeghe, C., Segers, K., Vanbellinghen, J.F., Ngendahayo, L., Rusingiza, E.K., Mutwa, P.R., Rulisa, S., Koulischer, L., *et al.* (2009). Genetic analysis of Rwandan patients with cystic fibrosis-like symptoms: identification of novel cystic fibrosis transmembrane conductance regulator and epithelial sodium channel gene variants. Chest *135*, 1233-1242.
Nabbout, R., Depienne, C., Chiron, C., and Dulac, O. (2011). Protocadherin 19 mutations in girls with infantile-onset epilepsy. Neurology *76*, 1193-1194; author reply 1194.

Nagae, S., Tanoue, T., and Takeichi, M. (2007). Temporal and spatial expression profiles of the Fat3 protein, a giant cadherin molecule, during mouse development. Dev Dyn *236*, 534-543.
Naisbitt, S., Kim, E., Tu, J.C., Xiao, B., Sala, C., Valtschanoff, J., Weinberg, R.J., Worley, P.F., and Sheng, M. (1999). Shank, a novel family of postsynaptic density proteins that binds to the NMDA receptor/PSD-95/GKAP complex and cortactin. Neuron *23*, 569-582.
Nakamura, T., Komiya, M., Sone, K., Hirose, E., Gotoh, N., Morii, H., Ohta, Y., and Mori, N. (2002). Grit, a GTPase-activating protein for the Rho family, regulates neurite extension through association with the TrkA receptor and N-Shc and CrkL/Crk adapter molecules. Mol Cell Biol *22*, 8721-8734.
Nakao, S., Platek, A., Hirano, S., and Takeichi, M. (2008). Contact-dependent promotion of cell migration by the OL-protocadherin-Nap1 interaction. J Cell Biol *182*, 395-410.
Nakazawa, T., Watabe, A.M., Tezuka, T., Yoshida, Y., Yokoyama, K., Umemori, H., Inoue, A., Okabe, S., Manabe, T., and Yamamoto, T. (2003). p250GAP, a novel brain-enriched GTPase-activating protein for Rho family GTPases, is involved in the N-methyl-d-aspartate receptor signaling. Mol Biol Cell *14*, 2921-2934.
Nasu-Nishimura, Y., Jaffe, H., Isaac, J.T., and Roche, K.W. (2010). Differential regulation of kainate receptor trafficking by phosphorylation of distinct sites on GluR6. J Biol Chem *285*, 2847-2856.
Negri, S., Oberson, A., Steinmann, M., Sauser, C., Nicod, P., Waeber, G., Schorderet, D.F., and Bonny, C. (2000). cDNA cloning and mapping of a novel islet-brain/JNK-interacting protein. Genomics *64*, 324-330.
Nguyen, A.W., and Daugherty, P.S. (2005). Evolutionary optimization of fluorescent proteins for intracellular FRET. Nat Biotechnol *23*, 355-360.
Nishi, M., Mizushima, A., Nakagawara, K., and Takeshima, H. (2000). Characterization of human junctophilin subtype genes. Biochem Biophys Res Commun *273*, 920-927.
Nishimura, K., Yoshihara, F., Tojima, T., Ooashi, N., Yoon, W., Mikoshiba, K., Bennett, V., and Kamiguchi, H. (2003). L1-dependent neuritogenesis involves ankyrinB that mediates L1-CAM coupling with retrograde actin flow. J Cell Biol *163*, 1077-1088.
Nishimura, Y., Shimojima, M., Tano, Y., Miyamura, T., Wakita, T., and Shimizu, H. (2009). Human P-selectin glycoprotein ligand-1 is a functional receptor for enterovirus 71. Nat Med *15*, 794-797.
Nishisho, I., Nakamura, Y., Miyoshi, Y., Miki, Y., Ando, H., Horii, A., Koyama, K., Utsunomiya, J., Baba, S., and Hedge, P. (1991). Mutations of chromosome 5q21 genes in FAP and colorectal cancer patients. Science *253*, 665-669.
Nomoto, H., Yonezawa, T., Itoh, K., Ono, K., Yamamoto, K., Oohashi, T., Shiraga, F., Ohtsuki, H., and Ninomiya, Y. (2003). Molecular cloning of a novel transmembrane protein MOLT expressed by mature oligodendrocytes. J Biochem *134*, 231-238.
O'Roak, B.J., Deriziotis, P., Lee, C., Vives, L., Schwartz, J.J., Girirajan, S., Karakoc, E., Mackenzie, A.P., Ng, S.B., Baker, C., *et al.* (2011). Exome sequencing in sporadic autism spectrum disorders identifies severe de novo mutations. Nat Genet *43*, 585-589.
Oda, H., Imai, Y., Nakatsuru, Y., Hata, J., and Ishikawa, T. (1996). Somatic mutations of the APC gene in sporadic hepatoblastomas. Cancer Res *56*, 3320-3323.

Oguri, M., Kato, K., Yokoi, K., Yoshida, T., Watanabe, S., Metoki, N., Yoshida, H., Satoh, K., Aoyagi, Y., Nozawa, Y., *et al.* (2010). Assessment of a polymorphism of SDK1 with hypertension in Japanese Individuals. Am J Hypertens *23*, 70-77.
Oh-hashi, K., Naruse, Y., Amaya, F., Shimosato, G., and Tanaka, M. (2003). Cloning and characterization of a novel GRP78-binding protein in the rat brain. J Biol Chem *278*, 10531-10537.
Ohi, K., Hashimoto, R., Nakazawa, T., Okada, T., Yasuda, Y., Yamamori, H., Fukumoto, M., Umeda-Yano, S., Iwase, M., Kazui, H., *et al.* (2012). The p250GAP gene is associated with risk for schizophrenia and schizotypal personality traits. PLoS One *7*, e35696.
Olszewski, P.K., Rozman, J., Jacobsson, J.A., Rathkolb, B., Stromberg, S., Hans, W., Klockars, A., Alsio, J., Riserus, U., Becker, L., *et al.* (2012). Neurobeachin, a regulator of synaptic protein targeting, is associated with body fat mass and feeding behavior in mice and body-mass index in humans. PLoS Genet *8*, e1002568.
Pajusola, K., Aprelikova, O., Korhonen, J., Kaipainen, A., Pertovaara, L., Alitalo, R., and Alitalo, K. (1992). FLT4 receptor tyrosine kinase contains seven immunoglobulin-like loops and is expressed in multiple human tissues and cell lines. Cancer Res *52*, 5738-5743.
Park, H.K., Park, H.W., Jeon, S.G., Shin, E.S., Gho, Y.S., Cho, S.H., Kim, Y.Y., and Kim, Y.K. (2008). Distinct association of genetic variations of vascular endothelial growth factor, transforming growth factor-beta, and fibroblast growth factor receptors with atopy and airway hyperresponsiveness. Allergy *63*, 447-453.
Parnis, A., Rawet, M., Regev, L., Barkan, B., Rotman, M., Gaitner, M., and Cassel, D. (2006). Golgi localization determinants in ArfGAP1 and in new tissue-specific ArfGAP1 isoforms. J Biol Chem *281*, 3785-3792.
Payne, J.A., Xu, J.C., Haas, M., Lytle, C.Y., Ward, D., and Forbush, B., 3rd (1995). Primary structure, functional expression, and chromosomal localization of the bumetanide-sensitive Na-K-Cl cotransporter in human colon. J Biol Chem *270*, 17977-17985.
Pedrosa, E., Stefanescu, R., Margolis, B., Petruolo, O., Lo, Y., Nolan, K., Novak, T., Stopkova, P., and Lachman, H.M. (2008). Analysis of protocadherin alpha gene enhancer polymorphism in bipolar disorder and schizophrenia. Schizophr Res *102*, 210-219.
Perletti, L., Talarico, D., Trecca, D., Ronchetti, D., Fracchiolla, N.S., Maiolo, A.T., and Neri, A. (1997). Identification of a novel gene, PSD, adjacent to NFKB2/lyt-10, which contains Sec7 and pleckstrin-homology domains. Genomics *46*, 251-259.
Peters, L.L., John, K.M., Lu, F.M., Eicher, E.M., Higgins, A., Yialamas, M., Turtzo, L.C., Otsuka, A.J., and Lux, S.E. (1995). Ank3 (epithelial ankyrin), a widely distributed new member of the ankyrin gene family and the major ankyrin in kidney, is expressed in alternatively spliced forms, including forms that lack the repeat domain. J Cell Biol *130*, 313-330.
Petralia, R.S., Wang, Y.X., and Wenthold, R.J. (1994). The NMDA receptor subunits NR2A and NR2B show histological and ultrastructural localization patterns similar to those of NR1. J Neurosci *14*, 6102-6120.
Philibert, R.A., Winfield, S.L., Sandhu, H.K., Martin, B.M., and Ginns, E.I. (2000). The structure and expression of the human neuroligin-3 gene. Gene *246*, 303-310.

Pinto, D., Pagnamenta, A.T., Klei, L., Anney, R., Merico, D., Regan, R., Conroy, J., Magalhaes, T.R., Correia, C., Abrahams, B.S., *et al.* (2010). Functional impact of global rare copy number variation in autism spectrum disorders. Nature *466*, 368-372.
Plowman, G.D., Culouscou, J.M., Whitney, G.S., Green, J.M., Carlton, G.W., Foy, L., Neubauer, M.G., and Shoyab, M. (1993). Ligand-specific activation of HER4/p180erbB4, a fourth member of the epidermal growth factor receptor family. Proc Natl Acad Sci U S A *90*, 1746-1750.
Potkin, S.G., Turner, J.A., Guffanti, G., Lakatos, A., Fallon, J.H., Nguyen, D.D., Mathalon, D., Ford, J., Lauriello, J., and Macciardi, F. (2009). A genome-wide association study of schizophrenia using brain activation as a quantitative phenotype. Schizophr Bull *35*, 96-108.
Prigmore, E., Ahmed, S., Best, A., Kozma, R., Manser, E., Segal, A.W., and Lim, L. (1995). A 68-kDa kinase and NADPH oxidase component p67phox are targets for Cdc42Hs and Rac1 in neutrophils. J Biol Chem *270*, 10717-10722.
Qin, S., Zhao, X., Pan, Y., Liu, J., Feng, G., Fu, J., Bao, J., Zhang, Z., and He, L. (2005). An association study of the N-methyl-D-aspartate receptor NR1 subunit gene (GRIN1) and NR2B subunit gene (GRIN2B) in schizophrenia with universal DNA microarray. Eur J Hum Genet *13*, 807-814.
Quintero-Rivera, F., Chan, A., Donovan, D.J., Gusella, J.F., and Ligon, A.H. (2007). Disruption of a synaptotagmin (SYT14) associated with neurodevelopmental abnormalities. Am J Med Genet A *143*, 558-563.
Rae, F.K., Hooper, J.D., Eyre, H.J., Sutherland, G.R., Nicol, D.L., and Clements, J.A. (2001). TTYH2, a human homologue of the Drosophila melanogaster gene tweety, is located on 17q24 and upregulated in renal cell carcinoma. Genomics *77*, 200-207.
Reiman, E.M., Webster, J.A., Myers, A.J., Hardy, J., Dunckley, T., Zismann, V.L., Joshipura, K.D., Pearson, J.V., Hu-Lince, D., Huentelman, M.J., *et al.* (2007). GAB2 alleles modify Alzheimer's risk in APOE epsilon4 carriers. Neuron *54*, 713-720.
Rivera, M.N., Kim, W.J., Wells, J., Driscoll, D.R., Brannigan, B.W., Han, M., Kim, J.C., Feinberg, A.P., Gerald, W.L., Vargas, S.O., *et al.* (2007). An X chromosome gene, WTX, is commonly inactivated in Wilms tumor. Science *315*, 642-645.
Rivera, M.N., Kim, W.J., Wells, J., Stone, A., Burger, A., Coffman, E.J., Zhang, J., and Haber, D.A. (2009). The tumor suppressor WTX shuttles to the nucleus and modulates WT1 activity. Proc Natl Acad Sci U S A *106*, 8338-8343.
Rodrigues, P., Furriol, J., Tormo, E., Ballester, S., Lluch, A., and Eroles, P. (2012). The single-nucleotide polymorphisms +936 C/T VEGF and -710 C/T VEGFR1 are associated with breast cancer protection in a Spanish population. Breast Cancer Res Treat *133*, 769-778.
Ronesi, J.A., Collins, K.A., Hays, S.A., Tsai, N.P., Guo, W., Birnbaum, S.G., Hu, J.H., Worley, P.F., Gibson, J.R., and Huber, K.M. (2012). Disrupted Homer scaffolds mediate abnormal mGluR5 function in a mouse model of fragile X syndrome. Nat Neurosci *15*, 431-440, S431.
Rot, S., Taubert, H., Bache, M., Greither, T., Wurl, P., Eckert, A.W., Schubert, J., Vordermark, D., and Kappler, M. (2011). A novel splice variant of the stem cell marker LGR5/GPR49 is correlated with the risk of tumor-related death in soft-tissue sarcoma patients. BMC Cancer *11*, 429.

Saez de Guinoa, J., Barrio, L., Mellado, M., and Carrasco, Y.R. (2011). CXCL13/CXCR5 signaling enhances BCR-triggered B-cell activation by shaping cell dynamics. Blood *118*, 1560-1569.
Sakuma, H., Ikeda, A., Oka, S., Kozutsumi, Y., Zanetta, J.P., and Kawasaki, T. (1997). Molecular cloning and functional expression of a cDNA encoding a new member of mixed lineage protein kinase from human brain. J Biol Chem *272*, 28622-28629.
Sato, D., Lionel, A.C., Leblond, C.S., Prasad, A., Pinto, D., Walker, S., O'Connor, I., Russell, C., Drmic, I.E., Hamdan, F.F., *et al.* (2012). SHANK1 Deletions in Males with Autism Spectrum Disorder. Am J Hum Genet *90*, 879-887.
Schiaffino, M.V., Bassi, M.T., Rugarli, E.I., Renieri, A., Galli, L., and Ballabio, A. (1995). Cloning of a human homologue of the Xenopus laevis APX gene from the ocular albinism type 1 critical region. Hum Mol Genet *4*, 373-382.
Schiffer, H.H., and Heinemann, S.F. (2007). Association of the human kainate receptor GluR7 gene (GRIK3) with recurrent major depressive disorder. Am J Med Genet B Neuropsychiatr Genet *144B*, 20-26.
Shekarabi, M., and Kennedy, T.E. (2002). The netrin-1 receptor DCC promotes filopodia formation and cell spreading by activating Cdc42 and Rac1. Mol Cell Neurosci *19*, 1-17.
Shiratsuchi, T., Nishimori, H., Ichise, H., Nakamura, Y., and Tokino, T. (1997). Cloning and characterization of BAI2 and BAI3, novel genes homologous to brain-specific angiogenesis inhibitor 1 (BAI1). Cytogenet Cell Genet *79*, 103-108.
Simon, D.B., Karet, F.E., Hamdan, J.M., DiPietro, A., Sanjad, S.A., and Lifton, R.P. (1996). Bartter's syndrome, hypokalaemic alkalosis with hypercalciuria, is caused by mutations in the Na-K-2Cl cotransporter NKCC2. Nat Genet *13*, 183-188.
Simpson, M.A., Irving, M.D., Asilmaz, E., Gray, M.J., Dafou, D., Elmslie, F.V., Mansour, S., Holder, S.E., Brain, C.E., Burton, B.K., *et al.* (2011). Mutations in NOTCH2 cause Hajdu-Cheney syndrome, a disorder of severe and progressive bone loss. Nat Genet *43*, 303-305.
Siu, K.Y., Yu, M.K., Wu, X., Zong, M., Roth, M.G., Chan, H.C., and Yu, S. (2011). The non-catalytic carboxyl-terminal domain of ARFGAP1 regulates actin cytoskeleton reorganization by antagonizing the activation of Rac1. PLoS One *6*, e18458.
Snapp, K.R., Heitzig, C.E., and Kansas, G.S. (2002). Attachment of the PSGL-1 cytoplasmic domain to the actin cytoskeleton is essential for leukocyte rolling on P-selectin. Blood *99*, 4494-4502.
Song, H., Tong, D., Cha, Z., and Bai, J. (2012). C-X-C chemokine receptor type 5 gene polymorphisms are associated with non-Hodgkin lymphoma. Mol Biol Rep *39*, 8629-8635.
Splawski, I., Shen, J., Timothy, K.W., Lehmann, M.H., Priori, S., Robinson, J.L., Moss, A.J., Schwartz, P.J., Towbin, J.A., Vincent, G.M., *et al.* (2000). Spectrum of mutations in long-QT syndrome genes. KVLQT1, HERG, SCN5A, KCNE1, and KCNE2. Circulation *102*, 1178-1185.
Srour, M., Riviere, J.B., Pham, J.M., Dube, M.P., Girard, S., Morin, S., Dion, P.A., Asselin, G., Rochefort, D., Hince, P., *et al.* (2010). Mutations in DCC cause congenital mirror movements. Science *328*, 592.
Steensma, D.P., Neiger, J.D., Porcher, J.C., Keats, J.J., Bergsagel, P.L., Dennis, T.R., Knudson, R.A., Jenkins, R.B., Santana-Davila, R., Kumar, R., *et al.* (2009).

Rearrangements and amplification of IER3 (IEX-1) represent a novel and recurrent molecular abnormality in myelodysplastic syndromes. Cancer Res *69*, 7518-7523.
Stefansson, H., Sigurdsson, E., Steinthorsdottir, V., Bjornsdottir, S., Sigmundsson, T., Ghosh, S., Brynjolfsson, J., Gunnarsdottir, S., Ivarsson, O., Chou, T.T., *et al.* (2002). Neuregulin 1 and susceptibility to schizophrenia. Am J Hum Genet *71*, 877-892.
Stephan, R., Gohl, C., Fleige, A., Klambt, C., and Bogdan, S. (2011). Membrane-targeted WAVE mediates photoreceptor axon targeting in the absence of the WAVE complex in Drosophila. Mol Biol Cell *22*, 4079-4092.
Strautnieks, S.S., Thompson, R.J., Gardiner, R.M., and Chung, E. (1996). A novel splice-site mutation in the gamma subunit of the epithelial sodium channel gene in three pseudohypoaldosteronism type 1 families. Nat Genet *13*, 248-250.
Strehl, S., Glatt, K., Liu, Q.M., Glatt, H., and Lalande, M. (1998). Characterization of two novel protocadherins (PCDH8 and PCDH9) localized on human chromosome 13 and mouse chromosome 14. Genomics *53*, 81-89.
Sundaresan, V., Roberts, I., Bateman, A., Bankier, A., Sheppard, M., Hobbs, C., Xiong, J., Minna, J., Latif, F., Lerman, M., *et al.* (1998). The DUTT1 gene, a novel NCAM family member is expressed in developing murine neural tissues and has an unusually broad pattern of expression. Mol Cell Neurosci *11*, 29-35.
Talkowski, M.E., Rosenfeld, J.A., Blumenthal, I., Pillalamarri, V., Chiang, C., Heilbut, A., Ernst, C., Hanscom, C., Rossin, E., Lindgren, A.M., *et al.* (2012). Sequencing chromosomal abnormalities reveals neurodevelopmental loci that confer risk across diagnostic boundaries. Cell *149*, 525-537.
Tariq, M., Belmont, J.W., Lalani, S., Smolarek, T., and Ware, S.M. (2011). SHROOM3 is a novel candidate for heterotaxy identified by whole exome sequencing. Genome Biol *12*, R91.
Tayler, T.D., and Garrity, P.A. (2003). Axon targeting in the Drosophila visual system. Curr Opin Neurobiol *13*, 90-95.
Triana-Baltzer, G.B., and Blank, M. (2006). Cytoplasmic domain of protocadherin-alpha enhances homophilic interactions and recognizes cytoskeletal elements. J Neurobiol *66*, 393-407.
Uhlen, M., Oksvold, P., Fagerberg, L., Lundberg, E., Jonasson, K., Forsberg, M., Zwahlen, M., Kampf, C., Wester, K., Hober, S., *et al.* (2010). Towards a knowledge-based Human Protein Atlas. Nat Biotechnol *28*, 1248-1250.
Walter, J.W., North, P.E., Waner, M., Mizeracki, A., Blei, F., Walker, J.W., Reinisch, J.F., and Marchuk, D.A. (2002). Somatic mutation of vascular endothelial growth factor receptors in juvenile hemangioma. Genes Chromosomes Cancer *33*, 295-303.
Wang, J.F., Zhang, X.F., and Groopman, J.E. (2001). Stimulation of beta 1 integrin induces tyrosine phosphorylation of vascular endothelial growth factor receptor-3 and modulates cell migration. J Biol Chem *276*, 41950-41957.
Wang, N.J., Sanborn, Z., Arnett, K.L., Bayston, L.J., Liao, W., Proby, C.M., Leigh, I.M., Collisson, E.A., Gordon, P.B., Jakkula, L., *et al.* (2011). Loss-of-function mutations in Notch receptors in cutaneous and lung squamous cell carcinoma. Proc Natl Acad Sci U S A *108*, 17761-17766.
Wang, Y., Kelber, J.A., Tran Cao, H.S., Cantin, G.T., Lin, R., Wang, W., Kaushal, S., Bristow, J.M., Edgington, T.S., Hoffman, R.M., *et al.* (2010). Pseudopodium-enriched

atypical kinase 1 regulates the cytoskeleton and cancer progression [corrected]. Proc Natl Acad Sci U S A *107*, 10920-10925.
Wang, Z.X. (1995). An exact mathematical expression for describing competitive binding of two different ligands to a protein molecule. FEBS Lett *360*, 111-114.
Watanabe, T., Wang, S., Noritake, J., Sato, K., Fukata, M., Takefuji, M., Nakagawa, M., Izumi, N., Akiyama, T., and Kaibuchi, K. (2004). Interaction with IQGAP1 links APC to Rac1, Cdc42, and actin filaments during cell polarization and migration. Dev Cell *7*, 871-883.
Wechezak, A.R., and Coan, D.E. (2005). Dvl2 silencing in postdevelopmental cells results in aberrant cell membrane activity and actin disorganization. J Cell Physiol *202*, 867-873.
Weinmaster, G., Roberts, V.J., and Lemke, G. (1992). Notch2: a second mammalian Notch gene. Development *116*, 931-941.
Williams, H.J., Craddock, N., Russo, G., Hamshere, M.L., Moskvina, V., Dwyer, S., Smith, R.L., Green, E., Grozeva, D., Holmans, P., *et al.* (2011). Most genome-wide significant susceptibility loci for schizophrenia and bipolar disorder reported to date cross-traditional diagnostic boundaries. Hum Mol Genet *20*, 387-391.
Wolverton, T., and Lalande, M. (2001). Identification and characterization of three members of a novel subclass of protocadherins. Genomics *76*, 66-72.
Wong, K., Ren, X.R., Huang, Y.Z., Xie, Y., Liu, G., Saito, H., Tang, H., Wen, L., Brady-Kalnay, S.M., Mei, L., *et al.* (2001). Signal transduction in neuronal migration: roles of GTPase activating proteins and the small GTPase Cdc42 in the Slit-Robo pathway. Cell *107*, 209-221.
Wymore, R.S., Gintant, G.A., Wymore, R.T., Dixon, J.E., McKinnon, D., and Cohen, I.S. (1997). Tissue and species distribution of mRNA for the IKr-like K+ channel, erg. Circ Res *80*, 261-268.
Wyszynski, M., Lin, J., Rao, A., Nigh, E., Beggs, A.H., Craig, A.M., and Sheng, M. (1997). Competitive binding of alpha-actinin and calmodulin to the NMDA receptor. Nature *385*, 439-442.
Yamaguchi, A., Urano, T., Goi, T., and Feig, L.A. (1997). An Eps homology (EH) domain protein that binds to the Ral-GTPase target, RalBP1. J Biol Chem *272*, 31230-31234.
Ying, J., Li, H., Seng, T.J., Langford, C., Srivastava, G., Tsao, S.W., Putti, T., Murray, P., Chan, A.T., and Tao, Q. (2006). Functional epigenetics identifies a protocadherin PCDH10 as a candidate tumor suppressor for nasopharyngeal, esophageal and multiple other carcinomas with frequent methylation. Oncogene *25*, 1070-1080.
Yu, J.S., Koujak, S., Nagase, S., Li, C.M., Su, T., Wang, X., Keniry, M., Memeo, L., Rojtman, A., Mansukhani, M., *et al.* (2008). PCDH8, the human homolog of PAPC, is a candidate tumor suppressor of breast cancer. Oncogene *27*, 4657-4665.
Zamorano-Leon, J.J., Yanez, R., Jaime, G., Rodriguez-Sierra, P., Calatrava-Ledrado, L., Alvarez-Granada, R.R., Mateos-Caceres, P.J., Macaya, C., and Lopez-Farre, A.J. (2012). KCNH2 Gene Mutation: A Potential Link Between Epilepsy and Long QT-2 Syndrome. J Neurogenet.
Zeggini, E., Scott, L.J., Saxena, R., Voight, B.F., Marchini, J.L., Hu, T., de Bakker, P.I., Abecasis, G.R., Almgren, P., Andersen, G., *et al.* (2008). Meta-analysis of genome-wide

association data and large-scale replication identifies additional susceptibility loci for type 2 diabetes. Nat Genet *40*, 638-645.
Zhang, H., Maximov, A., Fu, Y., Xu, F., Tang, T.S., Tkatch, T., Surmeier, D.J., and Bezprozvanny, I. (2005). Association of CaV1.3 L-type calcium channels with Shank. J Neurosci *25*, 1037-1049.
Zhao, C., Yu, D.H., Shen, R., and Feng, G.S. (1999). Gab2, a new pleckstrin homology domain-containing adapter protein, acts to uncouple signaling from ERK kinase to Elk-1. J Biol Chem *274*, 19649-19654.

Figure S1. PCDH10 Cytoplasmic Tail Directly Interacts with the WRC, Related to Figure 1.

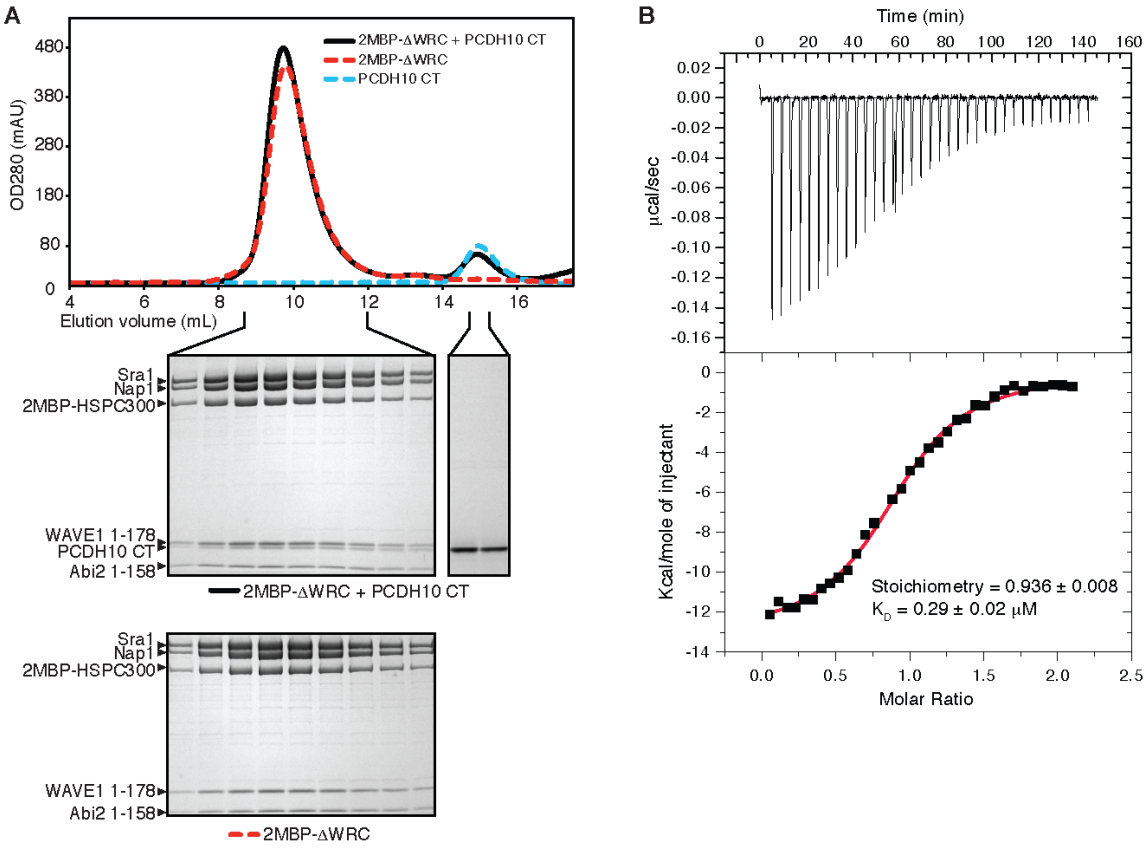

(A) Gel filtration chromatography of samples containing 4 µM 2MBP-ΔWRC and/or 15 µM mPCDH10 CT (879-1040). A 24-mL Superdex200 column was used and equilibrated with 20 mM Tris-HCl, 50 mM NaCl, 5% (w/v) glycerol, 1 mM DTT, pH 8.5. Commassie blue stained SDS-PAGE gels are shown for the corresponding fractions of the 2MBP-ΔWRC + PCDH10 CT samples (middle panel) and the 2MBP-ΔWRC samples (bottom panel).

(B) Isothermal titration calorimetry of PCDH10 CT (879-1040, 39.4 µM) titrated into

2MBP-miniWRC (4 μM) in buffer containing 20 mM Tris-HCl, 120 mM NaCl, 10% (w/v) glycerol, 1 mM EDTA, 1 mM DTT, pH 8.0 at 20 °C. Top and bottom panels (black squares) show raw and integrated heat from injections, respectively. The red curve in the bottom panel represents a fit of the integrated data to a single-site binding model.

Figure S2. Structural Comparison of the Apo-WRC and WIRS-bound WRC, Related to Figure 2.

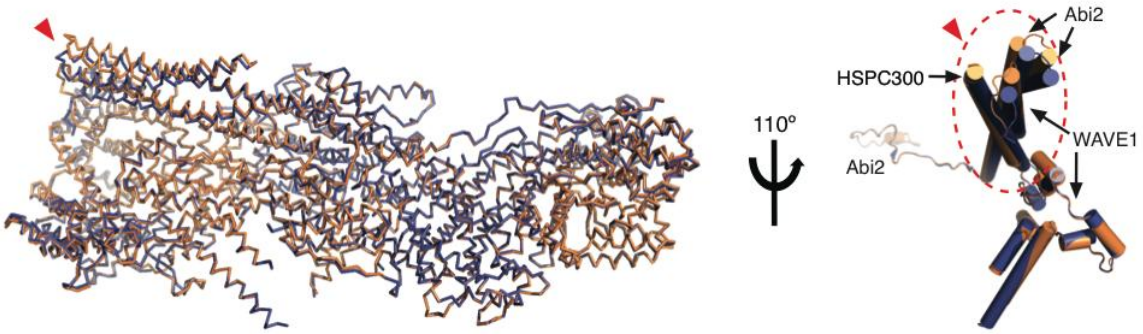

Cα superimposition of apo miniWRC (PDB ID: 3P8C, blue) and miniWRC bound to the WIRS peptide (orange) (Cα root mean squared deviations = 0.31 Å). The majority of the structures are essentially identical, except for small changes at the N-terminus of the WAVE1/Abi2/HSPC300 four-helix bundle (red arrows, and red dotted circle in the right panel). The HSPC300 helix has marginal changes, but the N-termini of the WAVE1 helix and the Abi2 helices shift by 3-7 Å. Whether this conformational change is induced by the WIRS binding or by crystal packing is not known.

Figure S3. Cytoplasmic Tails of PCDH10, PCDH17 and Neuroligin-1 Bind the WRC with Different Affinities, Related to Figure 6.

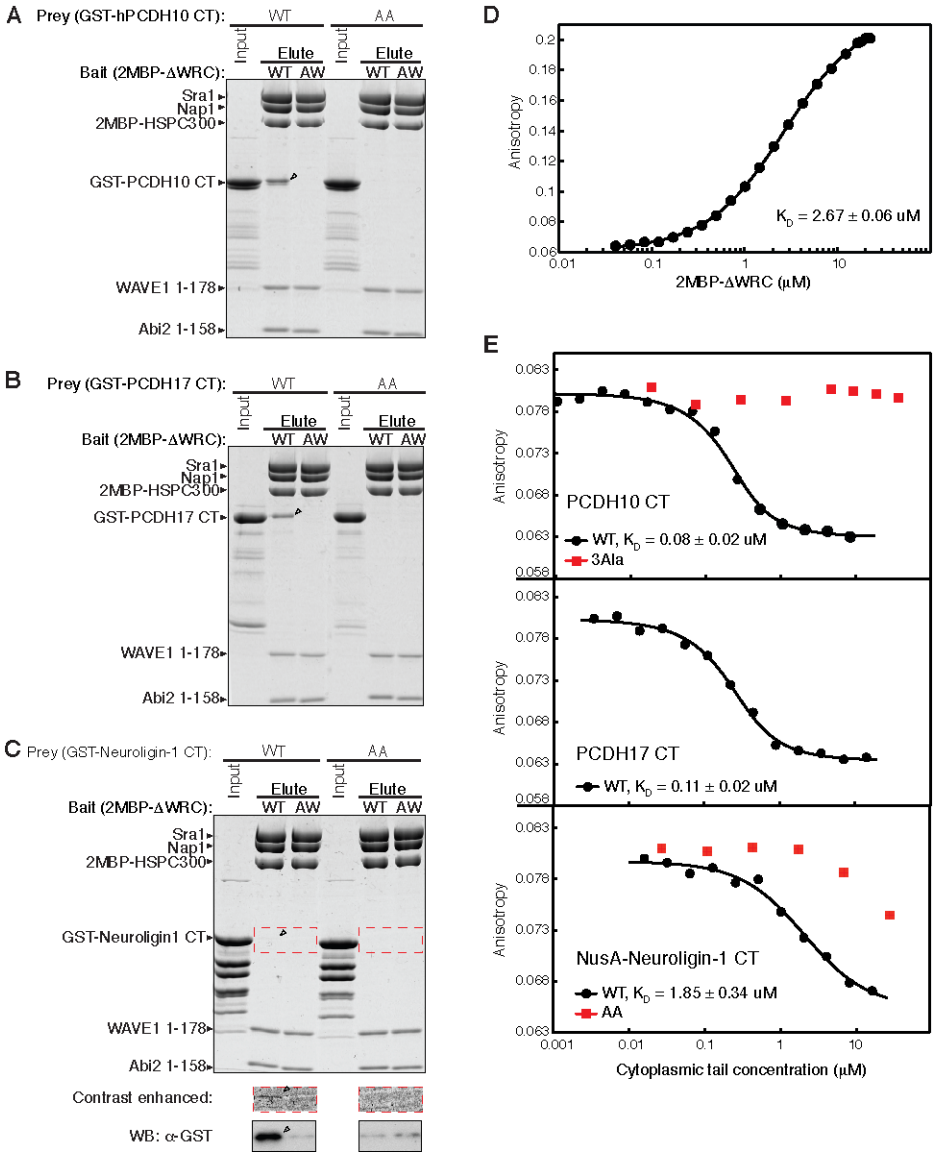

(A-C) Commassie blue stained SDS-PAGE gels show that the wild type 2MBP-ΔWRC (WT) but not a mutant (AW, or R106A/G110W) selectively retained GST-tagged cytoplasmic tails of PCDH10 (A), PCDH17 (B) and Neuroligin-1 (C) (WT for wild type, AA for tails with the conserved T/S-F in the WIRS motif mutated to A-A). Triangles

indicate proteins bound to the WRC. In (C) the boxed areas are contrast enhanced in the lower panels to better visualize bound GST-Neuroligin-1; bottom panel shows a western blot against the GST tag to further enhance the contrast.

(D) Fluorescence anisotropy direct binding assay, in which 2MBP-ΔWRC was added to FITC-labeled PCDH10 WIRS peptide. Changes in fluorescence anisotropy (black dots) were used to calculate K_D (solid line for the fitted curve, see also Extended Experimental Procedures).

(E) Fluorescence anisotropy competition assays, in which FITC labeled PCDH10 WIRS peptide pre-bound to 2MBP-ΔWRC was displaced by addition of indicated cytoplasmic tails of WIRS proteins. K_D was estimated by fitting to a complete solution for competitive binding to a single site on a receptor (Wang, 1995). Black fitted curves are for the wild type proteins (WT) and the red data points are for the mutant proteins (3Ala or F1000A/T1002A/F1003A for PCDH10 CT, and AA or T816A/F817A for NusA-tagged Neuroligin-1 CT). The binding buffer contains 10 mM Imidazole, 50 mM KCl, 1 mM $MgCl_2$, 1 mM EGTA, 20% (w/v) glycerol and 1mM DTT, pH 7.0, which may explain why the derived K_D of the PCDH10 CT was ~3-4 fold lower than the one from the isothermal titratration calorimetry assay (fig. S2) – the latter was performed with higher salt concentrations (120 mM NaCl).

Figure S4. Disruption of the WIRS Binding Site of the WRC Impairs Optic Lobe Development in Flies, Related to Figure 7.

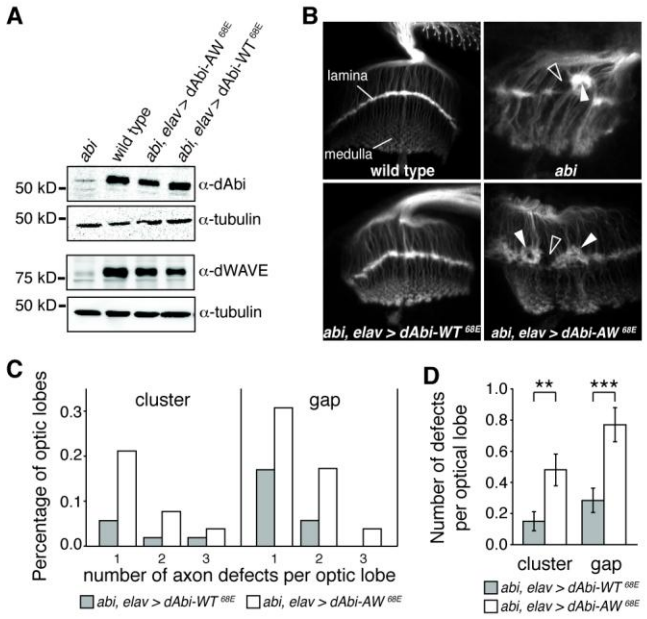

(A) Western blot analysis of brain lysate from third instar larvae of indicated genotypes is shown, supporting that re-expression of either the wild type Abi or the mutant dAbi-AW (AW for R118A/G122W-Abi) restored expression of WAVE and thus the WRC (Stephan et al., 2011).

(B) Representative third instar optic lobes of indicated genotypes stained with mAb24B10 (α-chaoptin; photoreceptor neurons), with empty arrows (for gaps) and white arrows (for clusters) denoting axonal organization defects. In the developing *Drosophila* visual system, extension of light sensing photoreceptor neuron axons from the eye to the brain is a highly stereotyped developmental process (Tayler and Garrity, 2003). In this process, photoreceptor axons are organized into many parallel non-overlapping columns and eventually terminate at two distinct neuropil areas, the lamina and the medulla (top

left). Loss of the WRC by knocking out either *abi*, *wave* or *kette/Nap1* leads to a similar disrupted development of the optic lobe, manifested by overlapping axons that create abnormal bundles and gaps in the lamina (Hummel et al., 2000; Stephan et al., 2011) (top right). These defects were nearly fully rescued by re-expressing the wild-type dAbi (bottom left) but were only partially rescued by the mutant (bottom right). Since the WRC is required in neurons of the target area to regulate photoreceptor axon targeting non-cell autonomously (Stephan et al., 2011), it remains unclear exactly how the WRC controls the targeting of retinal axons into the optic lobe.

(C-D) Quantification of the axonal defects represented in (B), n = 53 for wild type (WT, grey bars) and n = 52 for mutant with disrupted WIRS binding surface (AW, white bars) (n: number of analyzed optic lobes). Error bars represent SEM, p values were calculated by the Student's t-test (**: $p < 0.005$, ***: $p < 0.0005$). It is clear that in dAbi-AW rescued larval brains, significant numbers of abnormal clusters of fasciculating axons and large gaps in between were still observed in the lamina, in contrast to the near-complete rescue by dAbi wild type.

Table S1. Crystallography Data Collection and Refinement Statistics, Related to Figure 2.

	WRC/WIRS seleno*
Data collection	
Space group	$P2_12_12_1$
Cell dimensions	
a, b, c (Å)	97.49, 114.75, 323.61
α, β, γ (°)	90, 90, 90
Resolution (Å)	50-2.43 (2.48-2.43)#
R_{merge}	0.086 (0.54)
$I / \sigma I$	26 (1.84)
Completeness (%)	99.6 (98.8)
Redundancy	6.3 (4.4)
Refinement	
Resolution (Å)	19.98-2.43
No. reflections	262,551
R_{work} / R_{free}	18.4% / 20.9%
No. nonhydrogen atoms	
Protein	22,013
Water	746
B-factors	
Protein	60.4
Water	53.6
R.m.s. deviations	
Bond lengths (Å)	0.002
Bond angles (°)	0.589

*One crystal was used for the data collection.

#Values in parentheses are for the highest resolution shell.

Table S2. Predicted WIRS-containing Membrane or Membrane-associated Proteins.

See Excel spreadsheet.

Table S3. DNA Constructs and Peptides Used in this Study.

Construct name	Description*	Source or reference
Sra1	His6-Tev-hSra1 (1-1253, full length), His6-Tev finally removed	(Ismail et al., 2009)
Nap1	His6-Tev-hNap1 (1-1128, full length), His6-Tev finally removed	(Ismail et al., 2009)
ΔWAVE1	MBP-Tev-hWAVE1 (1-178), MBP-Tev finally removed	(Ismail et al., 2009)
miniWAVE1	MBP-Tev-hWAVE1 [(1-186)-(GGS)6-(485-559)], MBP-Tev finally removed	(Chen et al., 2010)
WAVE1-H6-FL [#1, 2]	MBP-Tev-hWAVE1 [(1-452)-HHHHHH-(457-559)], MBP-Tev finally removed	This study
VCA	hWAVE1(485-559)	(Ismail et al., 2009)
$WAVE1_{217}$ [#2]	MBP-Tev-hWAVE1 [(1-217)-(GGS)6-(485-559)], MBP-Tev finally removed	This study
ΔAbi2	MBP-Tev-hAbi2 (1-158), MBP-Tev finally removed	(Ismail et al., 2009)
HSPC300	MBP-Tev-hHSPC300 (1-79) (Full length), MBP-Tev finally removed	(Ismail et al., 2009)
2MBP-HSPC300	MBP-MBP-hHSPC300 (1-79) (Full length)	This study
2MBP-ΔWRC	Sra1 + Nap1 + ΔWAVE1 + ΔAbi2 + 2MBP-HSPC300	This study
$2MBP\text{-}\Delta WRC_{Y923A}$ [#3]	Sra1 (Y923A) + Nap1 + ΔWAVE1 + ΔAbi2 + 2MBP-HSPC300	This study
$2MBP\text{-}\Delta WRC_{L1090A}$ [#3]	Sra1 (L1090A) + Nap1 + ΔWAVE1 + ΔAbi2 + 2MBP-HSPC300	This study
$2MBP\text{-}\Delta WRC_{E1084A}$ [#3]	Sra1 (E1084A) + Nap1 + ΔWAVE1 + ΔAbi2 + 2MBP-HSPC300	This study
$2MBP\text{-}\Delta WRC_{R106A}$ [#3]	Sra1 + Nap1 + ΔWAVE1 + ΔAbi2 (R106A) + 2MBP-HSPC300	This study
$2MBP\text{-}\Delta WRC_{R106M}$ [#3]	Sra1 + Nap1 + ΔWAVE1 + ΔAbi2 (R106M) + 2MBP-HSPC300	This study
$2MBP\text{-}\Delta WRC_{R107A}$ [#3]	Sra1 + Nap1 + ΔWAVE1 + ΔAbi2 (R107A) + 2MBP-HSPC300	This study
$2MBP\text{-}\Delta WRC_{G110W}$ [#3]	Sra1 + Nap1 + ΔWAVE1 + ΔAbi2 (G110W) + 2MBP-HSPC300	This study
$2MBP\text{-}\Delta WRC_{AW}$ [#3]	Sra1 + Nap1 + ΔWAVE1 + ΔAbi2 (R106A/G110W) + 2MBP-HSPC300	This study
miniWRC	Sra1 + Nap1 + miniWAVE1 + ΔAbi2 + HSPC300	(Chen et al., 2010)
2MBP-miniWRC	Sra1 + Nap1 + miniWAVE1 + ΔAbi2 + 2MBP-HSPC300	This study
WRC217	Sra1 + Nap1 + $WAVE1_{217}$ + ΔAbi2 + HSPC300	This study
FL-WRC	Sra1 + Nap1 + WAVE1-H6-FL + ΔAbi2 + HSPC300	This study
dSra	His6-Tev-dSra (1-1291) (Full length), His6-Tev finally removed	(Ismail et al., 2009)
dNap	His6-Tev-dNap (1-1126) (Full length), His6-Tev finally removed	(Ismail et al., 2009)
dΔWAVE	MBP-Tev-dWAVE1 (1-181), MBP-Tev finally removed	(Ismail et al., 2009)

dΔAbi	MBP-Tev-dAbi (1-170), MBP-Tev finally removed	(Ismail et al., 2009)
2MBP-dHSPC300	MBP-MBP-dHSPC300 (1-76) (Full length)	(Ismail et al., 2009)
2MBP-dΔWRC	dSra + dNap + dΔWAVE + dΔAbi + 2MBP-dHSPC300	This study
2MBP-dΔWRC$_{AW}$ [#2]	dSra + dNap + dΔWAVE + dΔAbi (R118A/G122W) + 2MBP-dHSPC300	This study
Rac1	hRac1 Q61L full length	(Prigmore et al., 1995)
GST-Rac1	GST-Tev-hRac1 Q61L full length	(Prigmore et al., 1995)
GST-PCDH10 WIRS	GST-Tev-MERSFSTFGKE	This study
GST-PCDH10 WIRS $_{T1002A}$	GST-Tev-MERSFSAFGKE	This study
WIRS peptide	WGAERSFSTFGKEKA	Synthesized (Abgent)
WIRS 2Ala peptide	WGAERSFSAAGKEKA	Synthesized (Abgent)
FITC-WIRS peptide	FITC-GAERSFSTFGKEKA	Synthesized (UTSW)
Seleno-WIRS peptide	WGAERSM*STFGKEKA (M* = selenomethionine)	Synthesized (Abgent)
Peptide A	AVEYSDSEDDSEFDEVDWLE	Synthesized (UTSW)
GST-PCDH10 CT	GST-Tev-mPCDH10 (778-1040)	Openbiosystems (BU511004)
GST-PCDH10 CT with point mutations in WIRS [#4]	GST-PCDH10 CT with single point mutations E997A or R998A or S999(A, G, H P) or F1000(A, M, W, Y, S, G, T, N, P, E, V, K) or S1001(A, D, F, K, L, H, G, P) or T1002(A, S, V, G, C) or F1003(A, W, H, Y) or G1004(A, V, L, E, H) or K1005(A, G, R, M, F, E) or E1006A; or with multiple point mutations, with 997ERSFSTFGKE1006 replaced by 997AAAFATFGKA1006, or 997AAAFATFAKA1006, or 997AAAFATFGAA1006, or 997AAAFATFAAA1006, or 3Ala (F1000A/T1002A/F1003A).	This study
GST-PCDH10 (ΔCM1, ΔCM2) [#2]	GST-Tev-mPCDH10 [(778-906)-GGSEGGGSEGGSTGATSG-(925-939)-ASGSGGGSEGGSEGATS-(957-1040)]	This study
GST-PCDH10 CT$_{short}$	GST-Tev-mPCDH10 (879-1040)	This study
GST-hPCDH10 CT	GST-Tev-hPCDH10 (879-1040)	Openbiosystems (BC111560)
GST-hPCDH10 CT$_{short}$ AA[#3]	GST-Tev-hPCDH10 (879-1040), T1002A/F1003A	This study
GST-PCDH17 CT	GST-Tev-hPCDH17 (857-1159)	Openbiosystems (BC028165)
GST-PCDH17 CT AA[#3]	GST-Tev-hPCDH17 (857-1159), T1000A/F1001A	This study
GST-PCDH18 CT	GST-Tev-hPCDH18 (861-1135)	Openbiosystems (BC093815)
GST-PCDH19 CT	GST-Tev-mPCDH19 (875-1145)	Openbiosystems (BC118529)
GST-PCDH12 CT	GST-Tev-hPCDH12 (960-1184)	Openbiosystems (BC052973)
GST-PCDHα6 CT	GST-Tev-hPCDHa6 (728-919)	Openbiosystems (BC036674)
GST-PCDH8 CT	GST-Tev-hPCDH8 (915-1070)	Openbiosystems (BC036025)
GST-FAT1 CT	GST-Tev-mFAT1 (4215-4436)	Openbiosystems (BC049872)

GST-FAT3 CT[#5]	GST-Tev-mFAT3 (4185-4401)	Openbiosystems (CA318408)
GST-FAT3 CT_{mh}[#6]	GST-Tev-mFAT3 (4185-4386)-hFAT3 (4421-4589)	Openbiosystems (clone # LIFESEQ720863)
GST-LRIG3 CT	GST-Tev-hLRIG3 (841-1119)	Openbiosystems (BC126171)
GST-ROBO1 CT	GST-Tev-hROBO1 (886-1078)	Openbiosystems (BC115021)
GST-Neuroligin-1 CT	GST-Tev-hNeuroligin-1 (725-840)	Openbiosystems (BC032555)
GST-Neuroligin-1 CT AA[#3]	GST-Tev-hNeuroligin-1 (725-840), T816A/F817A	This study
NusA-Neuroligin-1 CT	NusA-Tev-hNeuroligin-1 (725-840)	This study
NusA-Neuroligin-1 CT AA[#3]	NusA-Tev-hNeuroligin-1 (725-840), T816A/F817A	This study
GST-Neuroligin-4X CT	GST-Tev-hNeuroligin-4X (721-817)	This study (cDNA from Nils Brose)
GST-Cav1.3 CT	GST-Tev-rCav1.3 (1914-2155)	This study (Zhang et al., 2005)
GST-BAI3 CT	GST-Tev-hBAI3 (1314-1502)	This study (Bolliger et al., 2011)
GST-mGluR5 CT	GST-Tev-rmGluR5 (912-1171)	This study (Ronesi et al., 2012)
GST-GluR6 CT	GST-Tev-rGluR6 (841-908)	This study (Nasu-Nishimura et al., 2010)
GST-P2RX7 CT	GST-Tev-hP2RX76 (359-519)	Openbiosystems (BC011913)
CD16-7-hPCDH10 CT[#7]	hCD16 (1-185)-hCD7 (146-203)-hPCDH10 (739-1040)-mCherry	This study (Blasutig et al., 2008)
CD16-7-hPCDH10 CT AA[#3, 7]	hCD16 (1-185)-hCD7 (146-203)-hPCDH10 (739-1040, T1002A/F1003A)-mCherry	This study (Blasutig et al., 2008)
CD16-7-PCDH17 CT[#7]	hCD16 (1-185)-hCD7 (146-203)-hPCDH17 (729-1159)-mCherry	This study (Blasutig et al., 2008)
CD16-7-PCDH17 CT AA[#3, 7]	hCD16 (1-185)-hCD7 (146-203)-hPCDH17 (729-1159, T1000A/F1001A)-mCherry	This study (Blasutig et al., 2008)
CD16-7-neuroligin1 CT[#7]	hCD16 (1-185)-hCD7 (146-203)-hNeuroligin1 (725-840)-mCherry	This study (Blasutig et al., 2008)
CD16-7-neuroligin1 CT AA[#3, 7]	hCD16 (1-185)-hCD7 (146-203)-hNeuroligin1 (725-840, T816A/F817A)-mCherry	This study (Blasutig et al., 2008)
Sra1-YPet[#8]	hSra1 (1-2353 full length)-(GGS)4-YPet	This study

Notes:

* Protein species: h for human, m for mouse, r for rat and d for drosophila. All sequences were confirmed by DNA sequencing.

#1. To facilitate purification of full-length hWAVE1 from bacterial expression, a His_6 tag was inserted into the unstructured poly-proline region for the MBP-tagged full-length hWAVE1. This allowed double-affinity purification first by amylose beads and then by Ni NTA beads to remove degraded materials.

#2. Inserting or replacing an internal sequence was done using overlapping PCR.

#3. Point mutations were made using QuikChange (Stratagene).

#4. To facilitate cloning, an XhoI and a HindIII restriction site were introduced flanking the WIRS site using QuikChange, producing a variant containing G995L/A996E/A1008L. These mutations did not seem to affect the binding of the cytoplasmic tail to the WRC. To introduce desired mutations to the WIRS, paired DNA oligos were designed to contain the mutations and produce compatible ends for XhoI and HindIII when annealed to form double-stranded oligos. The annealed oligos were directly ligated into the XhoI/HindIII double-digested GST-PCDH10 CT variant.

#5. The commercial cDNA clone lacked the c-terminus of the cytoplasmic tail (4402-4555) and had an internal insertion of 33 amino acids (NASIVTVIQLVNNVVDSIENEVSVMDQGQNYNR) between D4347 and A4349. The insertion does not contain a WIRS, and is conserved in the human FAT3 homologue, but not in rat. This construct contains both predicted WIRS motifs (Table S2).

#6. Two EST clones were assembled to generate a hybrid FAT3 full-length cytoplasmic tail containing 4185-4386 of mFAT3 and 4421-4589 of hFAT3 by overlapping PCR. The human FAT3 (4421-4589) sequence is 88% identical to the mouse FAT3.

#7. These vectors were modified from the pEGFP-N1 vector (Clontech). First the EGFP coding sequence was replaced by mCherry or YPet sequence between the BamHI and NotI sites. The CD16-CD7 coding sequence (Blasutig et al., 2008) was then inserted between NheI and XhoI of the new mCherry N1 vector. The coding sequences of different cytoplasmic tails were then subcloned in frame between XhoI and BamHI.

#8. First the pEGFP-N1 vector (Clontech) was modified by replacing the EGFP coding sequence with the YPet sequence between BamHI and NotI, with a $(GGS)_4$ linker inserted in frame following the BamHI site. The hSra1 coding sequence was then subcloned between XhoI and SacII. The resulting fusion coding sequence for hSra1-$(GGS)_4$-YPet was subcloned into the pGC-IRES vector (Costa et al., 2000) by replacing the sequences between two BamHI sites using the SLIC method (Li and Elledge, 2007).

Supplemental Figure 1

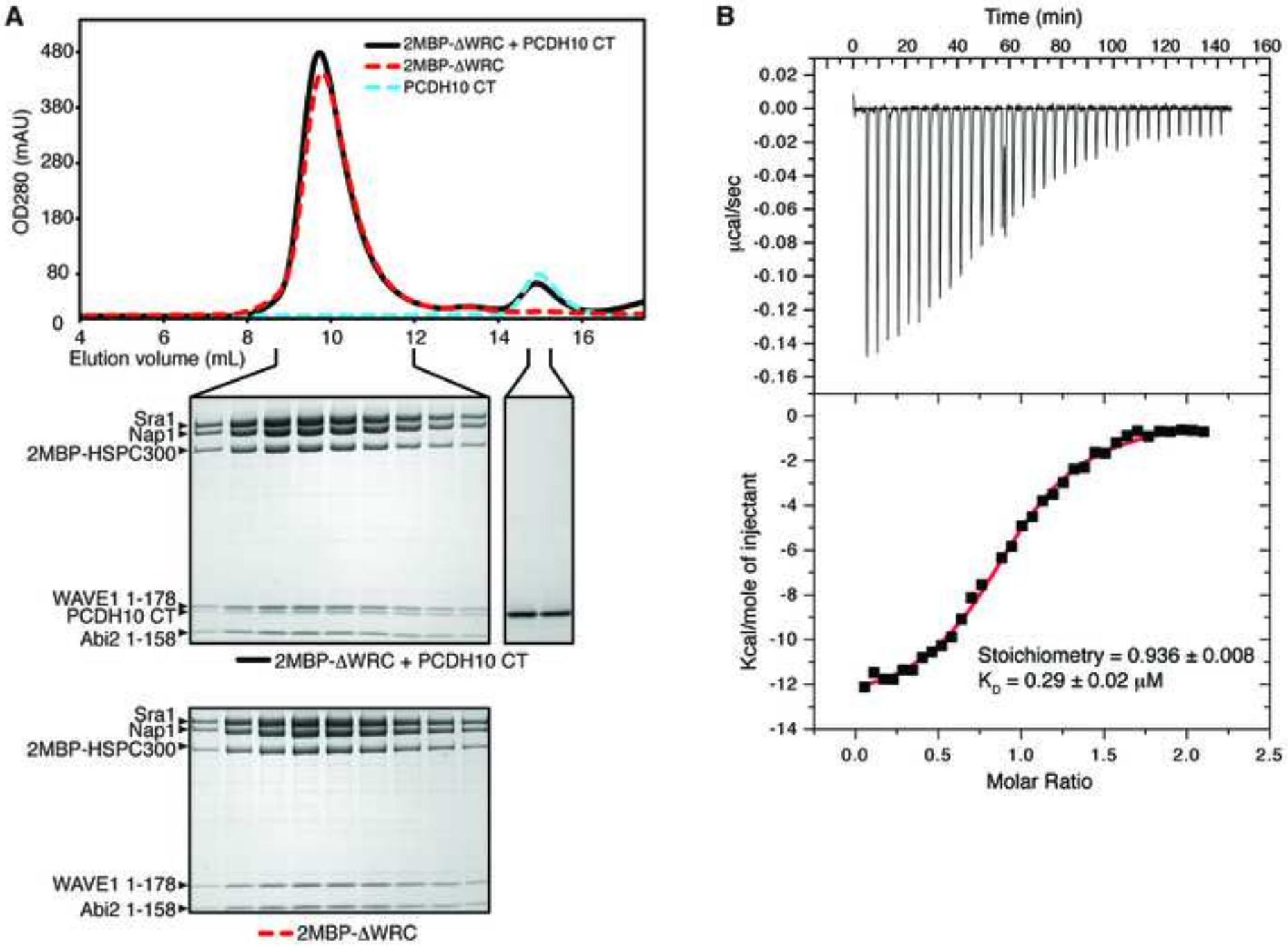

Supplemental Figure 2

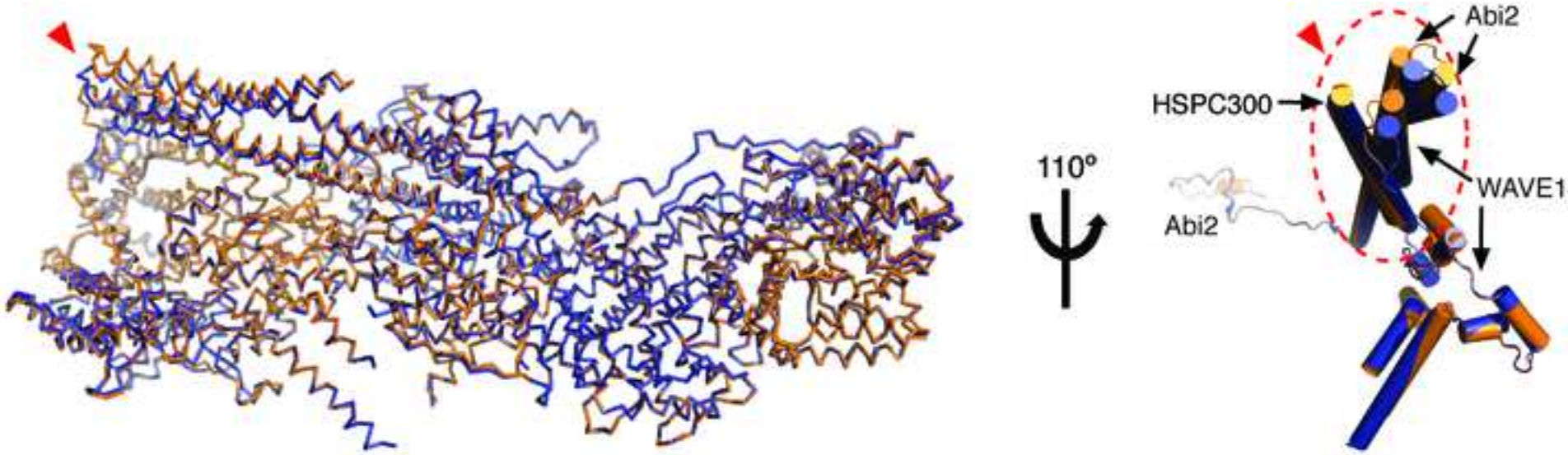

Supplemental Figure 3

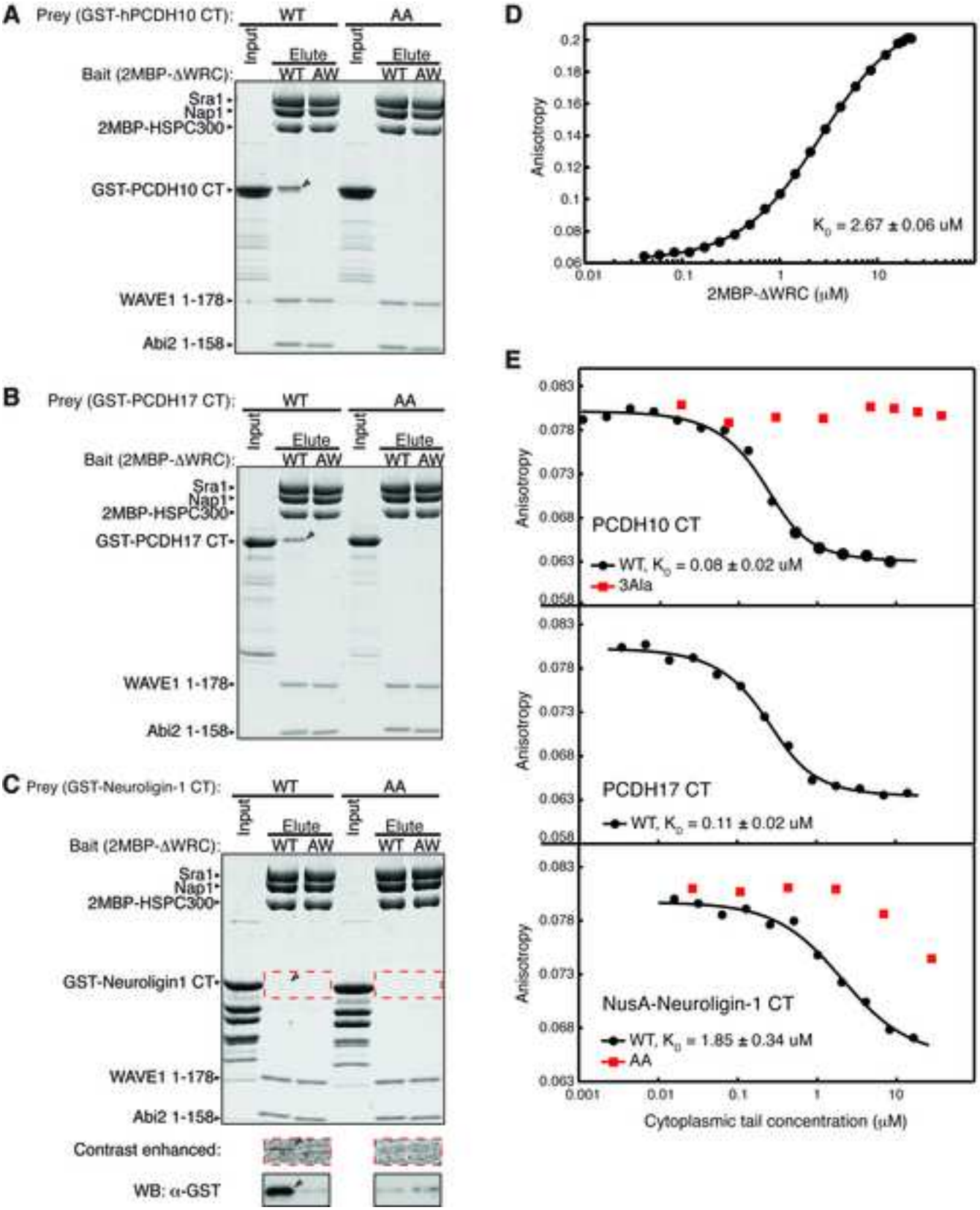

Supplemental Figure 4